



Variational estimates  
of black carbon  
emissions in the  
western United  
States

Y. Mao et al.

# Variational estimates of black carbon emissions in the western United States

Y. H. Mao<sup>1</sup>, Q. B. Li<sup>1,2</sup>, D. K. Henze<sup>3</sup>, Z. Jiang<sup>4,\*</sup>, D. B. A. Jones<sup>2,4</sup>, M. Kopacz<sup>5</sup>,  
C. He<sup>1</sup>, L. Qi<sup>1</sup>, M. Gao<sup>1</sup>, W.-M. Hao<sup>6</sup>, and K.-N. Liou<sup>1,2</sup>

<sup>1</sup>Department of Atmospheric and Oceanic Sciences, University of California, Los Angeles, CA 90095, USA

<sup>2</sup>Joint Institute for Regional Earth System Science and Engineering, University of California, Los Angeles, CA 90095, USA

<sup>3</sup>Department of Mechanical Engineering, University of Colorado, Boulder, CO 80309, USA

<sup>4</sup>Department of Physics, University of Toronto, Toronto, ON M5S 1A7, Canada

<sup>5</sup>NOAA Climate Program Office, Silver Spring, Maryland, 20910, USA

<sup>6</sup>Fire Sciences Laboratory, US Forest Service, Missoula, MT, 59808, USA

\* now at: Jet Propulsion Laboratory, California Institute of Technology, Pasadena, CA, 91109, USA

Received: 8 July 2014 – Accepted: 11 August 2014 – Published: 27 August 2014

Correspondence to: Q. B. Li (qli@atmos.ucla.edu)

Published by Copernicus Publications on behalf of the European Geosciences Union.

Title Page

Abstract

Introduction

Conclusions

References

Tables

Figures



Back

Close

Full Screen / Esc

Printer-friendly Version

Interactive Discussion



## Abstract

We estimate black carbon (BC) emissions in the Western United States (WUS) for July–September 2006 by inverting surface BC concentrations from the Interagency Monitoring of PROtected Visual Environment (IMPROVE) network using a global chemical transport model (GEOS-Chem) and its adjoint. Our best estimate of the BC emissions is 49.9 Gg at  $2^\circ \times 2.5^\circ$  (a factor of 2.1 increase) and 47.3 Gg at  $0.5^\circ \times 0.667^\circ$  (1.9 times increase). Model results now capture the observed major fire episodes with substantial bias reductions ( $\sim 35\%$  at  $2^\circ \times 2.5^\circ$  and  $\sim 15\%$  at  $0.5^\circ \times 0.667^\circ$ ). The emissions are  $\sim 20\text{--}50\%$  larger than those from our earlier analytical inversions (Mao et al., 2014). The discrepancy is especially drastic in the partitioning of anthropogenic vs. biomass burning emissions. The August biomass burning BC emissions are 4.6–6.5 Gg and anthropogenic BC emissions 8.6–12.8 Gg, varying with the model resolution, error specifications, and subsets of observations used. On average both increase twofold relative to the respective a priori emissions, in distinct contrast to the halving of the anthropogenic and tripling of the biomass burning emissions in the analytical inversions. We attribute these discrepancies to the inability of the inversion system, with limited spatiotemporal coverage of the IMPROVE observations, to effectively distinguish collocated anthropogenic and biomass burning emissions on model grid scales. This calls for concurrent measurements of other tracers of biomass burning and fossil fuel combustion (e.g., carbon monoxide and carbon isotopes). We find that the inversion system as is has sufficient information content to constrain the total emissions of BC on the model grid scales.

## 1 Introduction

Black carbon (BC) is directly emitted from the incomplete combustion of carbonaceous fuels (Bond et al., 2004). BC has substantial impacts on global climate because of its strong absorption of solar radiation (e.g., Horvath, 1993; Ramanathan and Carmichael,

## Variational estimates of black carbon emissions in the western United States

Y. Mao et al.

Title Page

Abstract

Introduction

Conclusions

References

Tables

Figures

◀

▶

◀

▶

Back

Close

Full Screen / Esc

Printer-friendly Version

Interactive Discussion





have been steadily decreasing as a result of effective emission controls (Novakov et al., 2003; Bond et al., 2007; Ramanathan and Carmichael, 2008).

Knowledge of the emissions of a chemical species is imperative for better understanding of its transport, distribution, and removal. Traditional bottom-up emission estimates generally depend on emission factors using socioeconomic, energy, land use, or environmental data (Bond et al., 2007, 2013; Lu et al., 2011). Top-down inverse method is able to improve the bottom-up emission estimates by minimizing an error-weighted least squares cost function (Rodgers, 2000). There are two methods to achieve the minimum of the cost function, the so-called analytical inversion and adjoint inversion (Kopacz et al., 2009, and references therein). The analytical method obtains an analytical solution by explicitly constructing a Jacobian matrix. However, the analytical method limits the number of the observations and the number of the sources and source regions that could be optimized because it is computationally expensive. Alternatively, the adjoint method seeks a numerical solution iteratively by using a suitable optimization algorithm (e.g., the conjugate gradient method) and is thus able to handle a very large number of observations and a large state vector resolved on a model grid scale.

Inverse modeling is suited for estimating emissions of unreactive or weakly reactive chemical species when their atmospheric concentrations are linearly or weakly non-linearly dependent on emissions (Müller and Stavrou, 2005). These species include but are not limited to carbon dioxide (e.g., Gloor et al., 1999; Chevallier et al., 2007; Pickett-Heaps et al., 2011), methane (e.g., Hein et al., 1997; Meirink et al., 2008; Wecht et al., 2012), and carbon monoxide (CO) (Stavrou and Müller, 2006; Arellano et al., 2004, 2006, 2007; Chevallier et al., 2009; Jones et al., 2009). Despite the non-linear complexities of the inversion system for short-lived tracer species, several studies have attempted to constrain emissions for nitrogen oxides (e.g., Martin et al., 2003, 2006; Chai et al., 2009; Lin et al., 2010; Zyrichidou et al., 2013), sulfur dioxide (Lee et al., 2012), and ammonia (Zhu et al., 2013; Paulot et al., 2014). The inverse method has also been used to constrain emission fluxes of aerosols, for instance, inorganic particu-

## Variational estimates of black carbon emissions in the western United States

Y. Mao et al.

Title Page

Abstract

Introduction

Conclusions

References

Tables

Figures

◀

▶

◀

▶

Back

Close

Full Screen / Esc

Printer-friendly Version

Interactive Discussion

late matter (Henze et al., 2009; Xu et al., 2013) and dust (Yumimoto et al., 2008; Wang et al., 2012).

A number of modeling studies have attempted to constrain and attribute BC emissions on regional to continental scales. Park et al. (2003) used multiple regressions to estimate annual mean emissions of primary carbonaceous aerosols in the US. Fu et al. (2012) and Wang et al. (2013) employed multiple regressions similar to that of Park et al. (2003) to estimate BC emission in China. Kopacz et al. (2011) used a global chemical transport model (CTM) and its adjoint to attribute the source regions of BC in the Himalayas and the Tibetan Plateau. Hakami et al. (2005) employed a continental-scale CTM (stretched over the Pacific basin) and its adjoint to estimate anthropogenic and biomass burning BC emissions during the Asian Pacific Regional Aerosol Characterization Experiment (ACE-Asia) (Huebert et al., 2003; Seinfeld et al., 2004). Mao et al. (2014) applied linear analytical inversions to optimize sources and source regions of BC in the western US.

Here we apply the variational (i.e., adjoint) inversion method (Henze et al., 2007, 2009) to improve estimates of BC emissions in the Western US (WUS, defined hereinafter as 30–50° N, 100–125° W for clarity) on model grid scales by inverting the surface BC concentrations from the Interagency Monitoring of PROtected Visual Environment (IMPROVE, Malm et al., 1994) network using the GEOS-Chem global 3-D CTM and its adjoint. We use the observations for 2006 from 69 mostly elevated mountainous sites in the WUS (Fig. 1). We focus our analysis on biomass burning emissions during the large fire season of July–September in the region (Mao et al., 2011, 2014).

## 2 GEOS-Chem and its adjoint

We apply the GEOS-Chem global 3-D CTM (Bey et al., 2001; with many updates thenceforth) to analyze IMPROVE BC data. Here we use GEOS-Chem version 8-02-01 (available at <http://geos-chem.org>) driven by GEOS-5 meteorological data. The detailed model configurations are as discussed by Mao et al. (2011, 2014). Global anthro-

### Variational estimates of black carbon emissions in the western United States

Y. Mao et al.

Title Page

Abstract

Introduction

Conclusions

References

Tables

Figures

◀

▶

◀

▶

Back

Close

Full Screen / Esc

Printer-friendly Version

Interactive Discussion



## Variational estimates of black carbon emissions in the western United States

Y. Mao et al.

Title Page

Abstract

Introduction

Conclusions

References

Tables

Figures

◀

▶

◀

▶

Back

Close

Full Screen / Esc

Printer-friendly Version

Interactive Discussion



pogenic emissions of BC are from Bond et al. (2007) with an updated seasonality from Park et al. (2003). Biomass burning emissions of BC are from the Global Fire Emissions Database version 2 (GFEDv2) emissions (Randerson et al., 2007; van der Werf et al., 2006), with improved spatiotemporal distributions using the active fire counts from the Moderate Resolution Imaging Spectroradiometer (MODIS) (Mao et al., 2014). For computational expediency, we conduct “offline” simulations of carbonaceous aerosols (Mao et al., 2011, and references therein) for 2006 at both  $2^\circ \times 2.5^\circ$  (globally) and  $0.5^\circ \times 0.667^\circ$  (nested over North America,  $40\text{--}140^\circ$  W longitudes,  $10\text{--}70^\circ$  N latitudes, cf. Fig. 1 in Wang et al., 2004) horizontal resolutions, following Mao et al. (2014). The first three months are used for initialization and we focus our analysis on July–September. Model results are sampled at the corresponding location and time of IMPROVE observations.

Henze et al. (2007, 2009) reported the development and first applications of the GEOS-Chem adjoint. A particular type of application of the adjoint is source attribution of chemical species at individual sites (e.g., Zhang et al., 2009; Kopacz et al., 2011; Parrington et al., 2012; Walker et al., 2012). Jiang et al. (2014a) reported the first nested-grid ( $0.5^\circ \times 0.667^\circ$ ) adjoint simulations of CO over North America. Here we use the adjoint of the “offline” simulation of BC at  $2^\circ \times 2.5^\circ$  (globally) and  $0.5^\circ \times 0.667^\circ$  (nested over North America). The computational cost of the adjoint simulation is 50 % greater than that of the corresponding forward simulation.

We validate the adjoint simulation of BC by comparing the adjoint gradients and the forward model sensitivities calculated using finite difference approximation (Henze et al., 2007; Zhu et al., 2013):

$$\Delta = \frac{J(\sigma + \delta\sigma) - J(\sigma)}{\delta\sigma} \quad (1)$$

where  $J$  is the cost function (Mao et al., 2014, and references therein), as discussed below in Sect. 3.1, and  $\sigma$  the scaling factor of BC emissions. We use  $\delta\sigma = 0.1$  here. Specifically we calculate the sensitivity of the BC mass at the surface with respect to the scaling factors of biomass burning and anthropogenic emissions of BC. Figure 2 shows the results from 1-week simulations for biomass burning (top panel) and anthropogenic

emissions (bottom panel) for August 2006. The adjoint and finite difference sensitivities are in excellent agreements ( $r \approx 1$ ), reaffirming the accuracy of the adjoint code.

### 3 Inversion approach

#### 3.1 The variational (adjoint) solution to the inverse problem

5 Consider the general problem of inferring emissions (state vector  $\mathbf{X}$ ) from a set of given observations (observation vector  $\mathbf{Y}$ ) with error  $\varepsilon$ . They are related via a forward model  $F$  as follows (Rodgers, 2000):

$$\mathbf{Y} = F(\mathbf{X}, b) + \varepsilon \quad (2)$$

10 where  $\mathbf{X}$  is the monthly biomass burning or anthropogenic emissions of BC in each model grid box in the present study,  $\mathbf{Y}$  the 24 h average surface BC concentrations from the 69 IMPROVE sites (Fig. 1),  $b$  the model variables not directly retrieved from the inversion,  $F$  the GEOS-Chem model, and  $\varepsilon$  the observation error (measurement and forward model errors). Based on Bayes' theorem and the assumption of Gaussian error distributions (Rodgers, 2000), the optimal or Maximum A Posteriori (MAP) solution for  
15  $\mathbf{X}$  given  $\mathbf{Y}$  is equivalent to finding the minimum of a cost function  $J(\mathbf{X})$ :

$$J(\mathbf{X}) = \frac{1}{2} \gamma_r (\mathbf{X} - \mathbf{X}_a)^T \mathbf{S}_a^{-1} (\mathbf{X} - \mathbf{X}_a) + \frac{1}{2} \sum_{i=0}^N [\mathbf{Y}_i - F(\mathbf{X}_i)]^T \mathbf{S}_\varepsilon^{-1} [\mathbf{Y}_i - F(\mathbf{X}_i)] = \gamma_r J_b + J_o \quad (3)$$

20 where  $\mathbf{X}_a$  and  $\mathbf{S}_a$  are the a priori emissions and the associated error covariance,  $\mathbf{S}_\varepsilon$  the observational error covariance, and  $\gamma_r$  the regularization parameter that adjusts the relative constraints by the observation term (i.e., the prediction term,  $J_o$ ) and the background term (i.e., the penalty term,  $J_b$ ) of the cost function (Hakami et al., 2005; Müller and Stavrakou, 2005; Henze et al., 2007; Kopacz et al., 2009). An observation term is

added to the cost function for each additional data source during the time interval  $[t_0, t_N]$ .

The adjoint approach seeks to minimize the cost function  $J(\mathbf{X})$  numerically and iteratively rather than analytically (Henze et al., 2007, 2009). Starting from an initial guess (i.e., the a priori emissions), the adjoint model efficiently computes the cost function gradients. A quasi-Newton L-BFGS algorithm (Liu and Nocedal, 1989) is then used to minimize the cost function iteratively, taking as input the cost function and its gradient. Such iterative optimizations using GEOS-Chem and its adjoint have been discussed in details previously (Henze et al., 2007, 2009; Kopacz et al., 2009, 2010).

### 3.2 Error specifications

A key aspect of inverse modeling is the specification of the error covariance matrices of variable parameters and observations (Palmer et al., 2003; Heald et al., 2004). We set the a priori and observation errors following Mao et al. (2014). We assume for separate inversions presented here an uncertainty of 30, 50, or 200 % for anthropogenic BC emissions and 300 or 500 % for biomass burning BC emissions. We assume that the a priori errors are spatially uncorrelated. The observation error includes the contributions from model error, representation error, and measurement error. We set the observation error at 30, 50, or 100 %. Setting these errors in relative terms can become problematic when the observed BC concentrations are vanishingly small. These small values tend to skew the inversion toward matching the minimal errors. We thus set an absolute error of  $0.04 \mu\text{g m}^{-3}$  based on the estimated observation errors. We showed previously that the combination of 50 % uncertainty for anthropogenic emissions, 500 % uncertainty for biomass burning emissions, and 30 % total observation error provided the best retrieval results in the analytical inversions (Mao et al., 2014). We adopt this set of error specifications in the standard inversion in the present study (Case 1, Table 1). The results are compared with those from the analytical inversions of Mao et al. (2014).

## Variational estimates of black carbon emissions in the western United States

Y. Mao et al.

Title Page

Abstract

Introduction

Conclusions

References

Tables

Figures

◀

▶

◀

▶

Back

Close

Full Screen / Esc

Printer-friendly Version

Interactive Discussion





### 3.3 Emission scaling factors $X/X_a$

We optimize here the scaling factors of emissions,  $X/X_a$ , rather than the actual emissions  $X$ , as a standard practice in inversion studies (Henze et al., 2009). Jiang et al. (2014b) have demonstrated that the form of the scaling factors in an adjoint inversion is crucial for the inversion to efficiently and rapidly converge to a solution. When the optimization is directly on the scaling factors expressed linearly as  $X/X_a$  (i.e., the cost function gradient is computed with respect to  $X/X_a$ ), the regions with strong a priori emissions tend to dominate the optimization, manifested in unrealistically large changes of emissions in these regions but limited variations in the regions with weak a priori emissions. Alternatively, when the optimization is instead on the logarithm of the scaling factors,  $\ln(X/X_a)$  (i.e., the cost function gradient is now computed with respect to  $\ln(X/X_a)$ ), the optimization can potentially result in an unbalanced convergence that is much faster for the regions with positive biases than for the regions with negative biases. Here we calculate cost function gradients with respect to a hybrid form of scaling factors (Jiang et al., 2014b). The hybrid form avoids the aforementioned limitations of optimizing the linear or logarithmic forms of the scaling factors. The resulting optimization converges equally efficiently for the regions with positive or negative biases.

### 3.4 The regularization parameter $\gamma_r$

The assumption that a priori errors are spatially uncorrelated hinges on the consideration that the spatial resolution of the CTM is much larger than the correlation length scale of the individual emission sources (Henze et al., 2009). However, the uncertainties of emissions from different model grid boxes (e.g.,  $\sim 200 \text{ km} \times 250 \text{ km}$  at  $2^\circ \times 2.5^\circ$ ) within a region (e.g., a country) are usually correlated (Stavrakou and Müller, 2006). Without explicitly enforcing these correlations, a regularization parameter, which ensures a smooth solution to the inversion, is often used to rectify the aforementioned inconsistency, by ensuring the a posteriori emissions remain sufficiently close to the a pri-

## Variational estimates of black carbon emissions in the western United States

Y. Mao et al.

Title Page

Abstract

Introduction

Conclusions

References

Tables

Figures

◀

▶

◀

▶

Back

Close

Full Screen / Esc

Printer-friendly Version

Interactive Discussion



## Variational estimates of black carbon emissions in the western United States

Y. Mao et al.

Title Page

Abstract

Introduction

Conclusions

References

Tables

Figures

◀

▶

◀

▶

Back

Close

Full Screen / Esc

Printer-friendly Version

Interactive Discussion



anthropogenic and biomass burning BC emissions from the standard adjoint inversion for August. The anthropogenic and biomass burning emissions are adjusted (higher or lower) alike in most grid boxes. Both the anthropogenic and biomass burning emissions increase twofold overall. The biomass burning emissions increase by varying factors (Table 1): 2.3 in the Rockies, 2.8 in California and the Southwest, and 1.5 in the Pacific Northwest – the regions are defined as in Mao et al. (2014).

The sensitivity of the cost function  $J(\mathbf{X})$  to the BC emissions is a useful metric for evaluating the inversions. Following Henze et al. (2009), we normalize the sensitivity as follows,

$$\frac{\partial J(\mathbf{X})}{\partial x_{m,i}} \frac{x_{m,i}}{J(\mathbf{X})} \quad (4)$$

It is the percentage of the cost function response to the fractional change in the BC emission source  $m$  (biomass burning, anthropogenic or total emissions) in model grid box  $i$ . As such, positive sensitivities are regions that BC emission reductions would improve model agreement with the observations. It is the opposite for negative sensitivities. The results for August are shown in Fig. 6. The inversions result in large reductions to both the positive and negative sensitivities ( $\sim 90\%$  on average at  $2^\circ \times 2.5^\circ$  and  $0.5^\circ \times 0.667^\circ$ ). The largest negative sensitivities to biomass burning emissions are in Washington, Ohio, Idaho, and California, where the sensitivities decrease significantly after the inversions.

### 4.1 Sensitivity analyses

Here we examine the sensitivity of the adjoint inversions to error specifications, choice of observations, collocated emissions, and the model resolution. These sensitivity analyses also provide a measure of the robustness of the inversions (Mao et al., 2014). For that purpose we conduct adjoint inversions at  $2^\circ \times 2.5^\circ$  and  $0.5^\circ \times 0.667^\circ$  (Cases 2–8, Table 1) in addition to the standard inversion (Case 1), with assorted a priori and observation errors, different subsets of the IMPROVE data, and collocated anthropogenic

and biomass burning emissions. The results are compared and contrasted with those from the standard adjoint inversion in the discussions hereafter, unless stated otherwise. We find that the inversions generally show comparable and consistent results with those from the standard inversion. The ensemble a posteriori biomass burning emissions (Cases 1–8) are 4.6–6.5 Gg (a factor of 1.7–2.3 relative to the a priori) and anthropogenic emissions 8.6–12.8 Gg (a factor of 1.5–2.2 increase).

#### 4.1.1 Error specifications

We first conduct adjoint inversions (Cases 2–5) to examine the sensitivity of the inversions to the a priori and observation errors. The a posteriori emissions are 3% lower when we reduce the uncertainty of the a priori biomass burning emissions from 500 to 300% (Case 2). Reducing the uncertainty of the a priori anthropogenic emissions from 50 to 30% brings no appreciable change to the a posteriori emissions (Case 3). Quadrupling that uncertainty (from 50 to 200%) increases the a posteriori emissions by 10% (Case 4). We find that the inversions are more sensitive to the observation error than the a priori error. For instance, an increase from 30 to 100% of the observation error (Case 5) results in a 16% decrease in the a posteriori emissions.

#### 4.1.2 Choices of observations

A robust inversion critically relies on the spatiotemporal coverage of the observations. Gloor et al. (1999) investigated the minimum number of observational sites needed for 10–20 regions in analytical inversions of carbon dioxide. They found that about 10 sites were needed per region. For BC, the number of site is usually fewer than 10 per region. Hakami et al. (2005) employed an adjoint approach to optimize ~ 20000 variables constrained by only ~ 1000 BC observations during ACE-Asia (Huebert et al., 2003; Seinfeld et al., 2004). In this study, we use ~ 690 observations to constrain ~ 600 variables at  $2^\circ \times 2.5^\circ$  and ~ 10000 at  $0.5^\circ \times 0.667^\circ$ .

### Variational estimates of black carbon emissions in the western United States

Y. Mao et al.

Title Page

Abstract

Introduction

Conclusions

References

Tables

Figures

◀

▶

◀

▶

Back

Close

Full Screen / Esc

Printer-friendly Version

Interactive Discussion



## Variational estimates of black carbon emissions in the western United States

Y. Mao et al.

Title Page

Abstract

Introduction

Conclusions

References

Tables

Figures

◀

▶

◀

▶

Back

Close

Full Screen / Esc

Printer-friendly Version

Interactive Discussion



Here we conduct two inversions to probe the sensitivity of the inversion to observations by using subsets of the IMPROVE data and comparing the results with those from the standard inversion (Case 1). In the inversion (Case 6), we set aside 13 ( $\sim 20\%$  of the 69) sites with  $\chi^2 > 1.5$  and large model-observation departure ( $> 0.5 \mu\text{g m}^{-3}$ ).  $\chi^2$  is calculated as the square of the ratio of the difference between modeled and observed surface BC concentrations to the observation accuracy. The measurements from these 13 sites are used as independent observations, whereas the measurements from the remaining 56 sites are used in the inversion. We find that the resulting a posteriori emissions (Fig. 7) are within 6% of those from Case 1 (Fig. 5). The emissions differ significantly only in  $\sim 10\%$  of the grid boxes, mainly in the Pacific Northwest and the Rockies. The resulting surface BC concentrations averaged over the 13 sites are within 15% between the two Cases. There is a  $\sim 15\%$  reduction in the mean bias of the surface BC concentrations (averaged over the 13 sites) for Case 6 and 20% for Case 1. In another inversion (not shown), we set aside four ( $\sim 5\%$  of the 69) sites with  $\chi^2 > 2$ . The results are also consistent with those from Case 1.

### 4.1.3 Collocated emissions

Mao et al. (2011) pointed out that biomass burning BC emissions were substantially underestimated in the WUS mountain ranges. There are large uncertainties in the temporal variation and spatial distribution of fire emissions (Langmann et al., 2009). Small fires are likely a major source of these uncertainties (Randerson et al., 2012). For instance, small fires can lead to large relative errors (50–100%) in burned area estimates (Korontzi et al., 2006; Giglio et al., 2006, 2010; McCarty et al., 2009; Roy and Boschetti, 2009).

Figure 8 shows monthly anthropogenic and biomass burning emissions in each  $2^\circ \times 2.5^\circ$  model grid box in the WUS. Collocated anthropogenic and biomass burning emissions are in most of the grid boxes. The anthropogenic emissions are larger than the biomass burning emissions in 80% of the grid boxes and still significant in the remaining 20%. We conduct an inversion (Case 7) to examine the ability of the





## Variational estimates of black carbon emissions in the western United States

Y. Mao et al.

Title Page

Abstract

Introduction

Conclusions

References

Tables

Figures

◀

▶

◀

▶

Back

Close

Full Screen / Esc

Printer-friendly Version

Interactive Discussion

We first conduct two inversions (Pseudos 1–2) to investigate the ability of the adjoint inversion system to distinguish collocated anthropogenic and biomass burning emissions. We consider two extreme scenarios: the pseudo observations are in every surface grid box (Pseudo 1) and in every grid box in the lowest 15 vertical layers (Pseudo 2). Other aspects of the two inversions remain the same as those of the standard inversion (Case 1). We find that the results are nearly indistinguishable. The a posteriori cost function is greatly reduced (by 95 % in Pseudo 1 and by 97 % in Pseudo 2). The a posteriori emissions both increase by exactly 5.6 Gg, fully recovering the added biomass burning emissions. However, the increase is uneven and not limited to the biomass burning emissions. The biomass burning emissions increase by a factor of 2.3 and anthropogenic emissions by a factor of 1.3. The inversions thus falsely impose larger anthropogenic emissions to minimize the large discrepancies between the model predictions and the pseudo observations. These two inversions show that even if there were observations everywhere, the inversion system would still lack the ability to effectively distinguish collocated biomass burning and anthropogenic emissions.

In the next three inversions (Pseudos 3–5), we examine the sensitivity of the inversion system to the constraints for anthropogenic vs. biomass burning emissions. Pseudos 3–5 are the same as Pseudo 1, but with several differences. The uncertainty of the anthropogenic emissions is reduced to 10 % in Pseudo 3. We assume that the anthropogenic emissions are perfect and leave them unchanged in Pseudo 4. In Pseudo 5, we let the biomass burning emissions remain unaltered. We find that the resulting a posteriori emissions from the former two (Pseudos 3 and 4) recover fully the added (biomass burning) emissions. The biomass burning emissions increase by a factor of 2.5 in Pseudo 3 (vs. 2.3 in Pseudo 1) and by a factor of 2.9 in Pseudo 4. However, the a posteriori emissions from Pseudo 5 increase by only 4.2 Gg, recovering just 75 % of the added (biomass burning) emissions. These results show yet again that the inversion system has difficulty to uniquely distinguish collocated biomass burning vs. anthropogenic emissions.





## Variational estimates of black carbon emissions in the western United States

Y. Mao et al.

Title Page

Abstract

Introduction

Conclusions

References

Tables

Figures

◀

▶

◀

▶

Back

Close

Full Screen / Esc

Printer-friendly Version

Interactive Discussion

sions, not only in the spatial distributions but also in the magnitudes (Figs. 5 and 10). In California, for example, the a posteriori biomass burning emissions at  $0.5^\circ \times 0.667^\circ$  increase in the adjoint inversion but decrease in the analytical inversion. The analytical inversions show factors of 3–5 increase of the biomass burning emissions and a  $\sim 50\%$  reduction of the anthropogenic emissions (Mao et al., 2014). In contrast, both the biomass burning and anthropogenic emissions in the adjoint inversions increase by two folds (Table 1). The total a posteriori emissions are rather comparable (within 20–50 %) between the two inversions.

Mao et al. (2014) have examined in detail the quality of the analytical inversions. The robustness of the analytical inversions and the relative consistency in the total a posteriori emissions from the two inversion methods therefore imply that the adjoint inversion results, at least the total emissions, are robust on the model grid scale. We will examine the robustness of the adjoint inversions further in Sect. 4.4. The large differences in the a posteriori anthropogenic and biomass burning emissions between the two inversion methods are largely because the inversion system has difficulty effectively distinguishing collocated biomass burning and anthropogenic emissions on model grid scales. As a result, the adjoint inversions tend to falsely impose larger anthropogenic emissions in the regions where the collocated biomass burning emissions are too low (Sects. 4.1.3 and 4.2). Jiang et al. (2011) also found that the adjoint inversion system is unable to distinguish CO emissions from collocated combustion and oxidation sources and they therefore lumped the two sectors in their inversions. The differences are also due to the large aggregation errors in the analytical inversions and the assumption of spatially uncorrelated a priori errors in the adjoint inversions (Sects. 3.2 and 3.4). The assumption that a priori errors are spatially uncorrelated hinges on the consideration that the spatial resolution of the CTM is much larger than the correlation length scale of the individual emission sources (Henze et al., 2009). However, the uncertainties of emissions from different model grid boxes (e.g.,  $\sim 200\text{ km} \times 250\text{ km}$  at  $2^\circ \times 2.5^\circ$ ) within a region (e.g., a country) are usually correlated (Stavrakou and Müller, 2006).

## Variational estimates of black carbon emissions in the western United States

Y. Mao et al.

Title Page

Abstract

Introduction

Conclusions

References

Tables

Figures

◀

▶

◀

▶

Back

Close

Full Screen / Esc

Printer-friendly Version

Interactive Discussion



We further separate the anthropogenic-dominated regions to examine the ability of the adjoint inversion system to constrain collocated emissions. In the regions where anthropogenic emissions are dominant, model surface BC concentrations are in good agreement with IMPROVE observations (Mao et al., 2011) and both the a posteriori anthropogenic and biomass burning emissions see substantial yet still relatively small increases. For example, the a posteriori anthropogenic and biomass burning emissions in Washington and Oregon increase by 39 and by 29%. However, in the regions where biomass burning emissions become more important but significantly underestimated, model surface BC concentrations are biased low and both the a posteriori anthropogenic and biomass burning emissions increase dramatically. For example, in Montana, Idaho, and Wyoming, the a posteriori anthropogenic and biomass burning emissions increase by factors of 2.2 and of 2.7. In California and Nevada, the a posteriori anthropogenic and biomass burning emissions increase both by a factor of 1.8. In Utah, Colorado, Arizona, and New Mexico, the corresponding emissions increase by factors of 1.8 and of 1.3.

### 4.4 Evaluation against observations

Model simulated surface BC concentrations with the a posteriori emissions show significant enhancements and largely reproduce both the synoptic variability and magnitudes of the observed surface BC concentrations, not only at individual sites (Fig. 11) but also on average at four altitude ranges (below 1, 1–2, 2–3, and above 3 km) (Fig. 12). For instance, model surface BC concentrations after the adjoint inversions capture the major fire episodes at Starkey, OR (45.2° N, 118.5° W, 1.26 km) and Lassen Volcanic, CA (40.5° N, 121.6° W, 1.73 km). The adjoint inversions at 0.5° × 0.667° provide better agreements with the observations than the analytical inversion results do at some sites, for example, Three Sisters, OR (44.3° N, 122.0° W, 0.89 km) and Pasayten, WA (48.4° N, 119.9° W, 1.63 km). At other sites, Jarbidge Wild, NV (41.9° N, 115.4° W, 1.87 km), for example, results from the analytical inversions are noticeably better. The two inversion results differ the most at 1–2 km altitudes and to a lesser degree at higher

## Variational estimates of black carbon emissions in the western United States

Y. Mao et al.

Title Page

Abstract

Introduction

Conclusions

References

Tables

Figures

◀

▶

◀

▶

Back

Close

Full Screen / Esc

Printer-friendly Version

Interactive Discussion

altitudes, for example, Bridger Wild, WY (43.0° N, 109.8° W, 2.63 km). The a posteriori emissions lead to an average bias reduction of  $\sim 50\%$  in the simulated surface BC concentrations at 1–2 km altitudes (Fig. 12). Model simulated surface BC concentrations with the a posteriori emissions from the adjoint inversions, especially at  $0.5^\circ \times 0.667^\circ$ , show substantial enhancements during major fire episodes. The enhancements are evident at all altitudes (up to  $0.2 \mu\text{g m}^{-3}$  at 1–2 km and  $0.1 \mu\text{g m}^{-3}$  at 2–3 km). The a posteriori emissions lead to large mean bias reductions (34 % at  $2^\circ \times 2.5^\circ$  and 20 % at  $0.5^\circ \times 0.667^\circ$  for August), as shown in Fig. 13. The frequency distributions of the bias of the 24 h average surface BC concentrations are Gaussian (Fig. 14), as expected. The inversions reduce both the mean (by  $\sim 35\%$  at  $2^\circ \times 2.5^\circ$  and  $\sim 15\%$  at  $0.5^\circ \times 0.667^\circ$  for July–September) and standard deviation of the biases.

Taylor diagram and skill score ( $S$ ) are useful measures of model accuracy. The diagram relates the centered root mean square error (RMSE), the pattern correlation ( $r$ ) and the standard deviation ( $\sigma$ ) of observations and model results (Taylor, 2001).  $S$  (0–1) increases with increasing correlations and as the modeled variance approaches the observed variance. Figure 15 presents the resulting diagram and skill scores of the observations and the multitude of model results. Model results with the a posteriori emissions are consistently in better agreement with the observations, especially using the nested model. The a posteriori emissions lead to higher  $r$  (by 11–48 % on average), larger  $\sigma$  (by 27–122 % on average), and lower centered RMSEs, thereby increasing the skill scores (by 43–221 %). The a posteriori emissions from the adjoint inversion at  $0.5^\circ \times 0.667^\circ$  show the smallest centered RMSE and largest  $r$ , whereas the a posteriori emissions from the analytical inversion at  $0.5^\circ \times 0.667^\circ$  show the largest  $\sigma$  and  $S$  values.

There are large uncertainties in the a posteriori emissions, as evident in the 20–30 % low bias in modeled surface BC concentrations. The uncertainties are partially because of the limitations of the inversion system, in both the nature of the inverse modeling and the spatiotemporal coverage of IMPROVE observations (see Sects. 4.1.3 and 4.2). The adjoint inversion system has sufficient information to constrain the total emissions of

BC, especially at the coarse resolution  $2^\circ \times 2.5^\circ$ . The inversion system however has difficulty in partitioning collocated anthropogenic vs. biomass burning emissions. Furthermore, comparing localized observations with coarse-resolution model results is inherently problematic (Mao et al., 2011; Fairlie et al., 2007). It is even more so because many of the IMPROVE sites are mountainous and the associated upslope flow is difficult to represent in a global model.

## 5 Summary and conclusions

We have applied variational (adjoint) inversions to derive top-down estimates of biomass burning and anthropogenic emissions of BC in the WUS for July–September 2006 by inverting the surface BC concentrations from the IMPROVE network. We conducted the inversions using the GEOS-Chem chemical transport model and its adjoint at  $2^\circ \times 2.5^\circ$  (globally) and  $0.5^\circ \times 0.667^\circ$  (nested over North America) horizontal resolutions. We examined the sensitivity of the inversions to a multitude of configurations of the inversion system including the model horizontal resolution, the a priori and observation errors, and subsets of the observations. The simulated surface BC concentrations with both the a priori and the a posteriori emissions were then evaluated with either all or subsets of the IMPROVE observations. Additionally, the results were compared and contrasted with those from our previous corresponding analytical inversions (Mao et al., 2014).

The a posteriori emissions of BC led to large reductions in the cost function ( $\sim 35\%$  at  $2^\circ \times 2.5^\circ$  and  $50\%$  at  $0.5^\circ \times 0.667^\circ$ ) and the normalized sensitivities of the cost function to the emissions ( $\sim 90\%$  on average). The total a posteriori emissions were 49.9 Gg at  $2^\circ \times 2.5^\circ$  (a factor of 2.1 increase) and 47.3 Gg at  $0.5^\circ \times 0.667^\circ$  (1.9 times increase) for July–September. The inversions with varying configurations showed consistent and comparable a posteriori emissions (within  $\sim 15\%$ ). The a posteriori biomass burning emissions were 4.6–6.5 Gg (1.7–2.3 times the a priori) for August and anthropogenic

### Variational estimates of black carbon emissions in the western United States

Y. Mao et al.

Title Page

Abstract

Introduction

Conclusions

References

Tables

Figures

⏪

⏩

◀

▶

Back

Close

Full Screen / Esc

Printer-friendly Version

Interactive Discussion



emissions were 8.6–12.8 Gg (1.5–2.2 times the a priori). The inversions were more sensitive to the observation error than to the a priori error.

The a posteriori emissions of BC differ considerably between the adjoint and analytical inversions, especially in the partitioning of anthropogenic vs. biomass burning emissions. The total was ~ 20–50 % larger in the adjoint inversions than in the analytical inversions. Both the biomass burning and anthropogenic emissions from the adjoint inversions doubled, whereas the analytical inversions showed factors of 3–5 increases in the former and ~ 50 % reductions in the latter. We attributed these differences to the inability of the adjoint inversion system to effectively distinguish collocated biomass burning and anthropogenic emissions on the model grid scales. That inability resulted in excessively large anthropogenic emissions in the regions where biomass burning emissions were underestimated.

The inversions with various pseudo observations indicated that observations of surface BC concentration covering half of the model grid boxes had sufficient information to constrain the total emissions of BC on the model grid scales. IMPROVE observations of BC have sufficient information to constrain the total BC emissions at the model grid scales, especially at  $2^\circ \times 2.5^\circ$ . The limitations of the adjoint inversion system, including the spatiotemporal coverage of the IMPROVE observations of BC, call for concurrent measurements of other combustion tracers (e.g., CO and carbon isotopes).

Modeled surface BC with the a posteriori emissions captured the major fire episodes observed at many sites, especially at 1–2 and 2–3 km altitudes, and provided better agreement with the observations, especially at  $0.5^\circ \times 0.667^\circ$ . The a posteriori emissions led to substantial bias reductions (~ 35 % on average at  $2^\circ \times 2.5^\circ$  and ~ 15 % at  $0.5^\circ \times 0.667^\circ$ ) in the simulated surface BC concentrations and significant increases in the Taylor skill scores (43 % at  $2^\circ \times 2.5^\circ$  and 164 % at  $0.5^\circ \times 0.667^\circ$ ).

*Acknowledgements.* This research was supported by NASA grant NNX09AF07G from the Atmospheric Chemistry Modeling and Analysis Program (ACMAP). The GEOS-Chem model is managed by the Atmospheric Chemistry Modeling group at Harvard University; support for the adjoint comes the Henze group at CU Boulder, which additionally recognizes support from EPA-

Variational estimates  
of black carbon  
emissions in the  
western United  
States

Y. Mao et al.

Title Page

Abstract

Introduction

Conclusions

References

Tables

Figures

◀

▶

◀

▶

Back

Close

Full Screen / Esc

Printer-friendly Version

Interactive Discussion



STAR grant 83503701 (this manuscript does not reflect official EPA agency views or policies). We thank Feng Deng and Ray Nassar for helpful discussions.

## References

- 5 Anenberg, S. C., Talgo, K., Arunachalam, S., Dolwick, P., Jang, C., and West, J. J.: Impacts of global, regional, and sectoral black carbon emission reductions on surface air quality and human mortality, *Atmos. Chem. Phys.*, 11, 7253–7267, doi:10.5194/acp-11-7253-2011, 2011.
- 10 Anenberg, S. C., Schwartz, J., Shindell, D., Amann, M., Faluvegi, G., Klimont, Z., Janssens-Maenhout, G., Pozzoli, L., Van Dingenen, R., Vignati, E., Emberson, L., Muller, N. Z., West, J. J., Williams, M., Demkine, V., Hicks, W. K., Kuylentierna, J., Raes, F., and Ramanathan, V.: Global air quality and health co-benefits of mitigating near-term climate change through methane and black carbon emission controls, *Environ. Health Persp.*, 120, 831–839, 2012.
- Arakawa, A. and Schubert, W. H.: Interaction of a cumulus cloud ensemble with the large-scale environment, Part I, *J. Atmos. Sci.*, 31, 674–701, 1974.
- 15 Arellano, A. F., Kasibhatla, P. S., Giglio, L., van der Werf, G. R., and Randerson, J. T.: Top-down estimates of global CO sources using MOPITT measurements, *Geophys. Res. Lett.*, 31, L01104, doi:10.1029/2003GL018609, 2004.
- Arellano, A. F., Kasibhatla, P. S., Giglio, L., van der Werf, G. R., Randerson, J. T., and Colatz, G. J.: Time-dependent inversion estimates of global biomass-burning CO emissions using Measurement of Pollution in the Troposphere (MOPITT) measurements, *J. Geophys. Res.*, 111, D09303, doi:10.1029/2005JD006613, 2006.
- 20 A. F. Arellano Jr., Raeder, K., Anderson, J. L., Hess, P. G., Emmons, L. K., Edwards, D. P., Pfister, G. G., Campos, T. L., and Sachse, G. W.: Evaluating model performance of an ensemble-based chemical data assimilation system during INTEX-B field mission, *Atmos. Chem. Phys.*, 7, 5695–5710, doi:10.5194/acp-7-5695-2007, 2007.
- 25 Bench, G.: Measurement of contemporary and fossil carbon contents of PM<sub>2.5</sub> aerosols: results from Turtleback Dome, Yosemite National Park, *Environ. Sci. Technol.*, 38, 2424–2427, 2004.
- Bench, G., Fallon, S., Schichtel, B., Malm, W., and McDade, C.: Relative contributions of fossil and contemporary carbon sources to PM<sub>2.5</sub> aerosols at nine Interagency Monitoring for Pro-
- 30

## Variational estimates of black carbon emissions in the western United States

Y. Mao et al.

Title Page

Abstract

Introduction

Conclusions

References

Tables

Figures

◀

▶

◀

▶

Back

Close

Full Screen / Esc

Printer-friendly Version

Interactive Discussion



**Variational estimates  
of black carbon  
emissions in the  
western United  
States**

Y. Mao et al.

Title Page

Abstract

Introduction

Conclusions

References

Tables

Figures

◀

▶

◀

▶

Back

Close

Full Screen / Esc

Printer-friendly Version

Interactive Discussion

tection of Visual Environments (IMPROVE) network sites, *J. Geophys. Res.*, 112, D10205, doi:10.1029/2006JD007708, 2007.

Bey, I., Jacob, D. J., Yantosca, R. M., Logan, J. A., Field, B. D., Fiore, A. M., Li, Q., Liu, H.-Y., Mickley, L. J., and Schultz, M. G.: Global modeling of tropospheric chemistry with assimilated meteorology: model description and evaluation, *J. Geophys. Res.*, 106, 23073–23095, 2001.

Bond, T. and Sun, H.: Can reducing black carbon emissions counteract global warming?, *Environ. Sci. Technol.*, 39, 5921–5926, 2005.

Bond, T. C., Streets, D. G., Yarber, K. F., Nelson, S. M., Woo, J.-H., and Klimont, Z.: A technology-based global inventory of black and organic carbon emissions from combustion, *J. Geophys. Res.*, 109, D14203, doi:10.1029/2003JD003697, 2004.

Bond, T. C., Bhardwaj, E., Dong, R., Jogani, R., Jung, S., Roden, C., Streets, D. G., and Trautmann, N. M.: Historical emissions of black and organic carbon aerosol from energy-related combustion, 1850–2000, *Global Biogeochem. Cy.*, 21, GB2018, doi:10.1029/2006GB002840, 2007.

Bond, T. C., Doherty, S. J., Fahey, D. W., Forster, P. M., Berntsen, T., DeAngelo, B. J., Flanner, M. G., Ghan, S., Kärcher, B., Koch, D., Kinne, S., Kondo, Y., Quinn, P. K., Sarofim, M. C., Schultz, M. G., Schulz, M., Venkataraman, C., Zhang, H., Zhang, S., Bellouin, N., Gutikunda, S. K., Hopke, P. K., Jacobson, M. Z., Kaiser, J. W., Klimont, Z., Lohmann, U., Schwarz, J. P., Shindell, D., Storelvmo, T., Warren, S. G., and Zender, C. S.: Bounding the role of black carbon in the climate system: a scientific assessment, *J. Geophys. Res.*, 118, 5380–5552, doi:10.1002/jgrd.50171, 2013.

Chai, T., Carmichael, G. R., Tang, Y., Sandu, A., Heckel, A., Richter, A., and Burrows, J. P.: Regional  $\text{NO}_x$  emission inversion through a four-dimensional variational approach using SCIAMACHY tropospheric  $\text{NO}_2$  column observations, *Atmos. Environ.*, 43, 5046–5055, 2009.

Chevallier, F., Brèon, F.-M., and Rayner, P. J.: Contribution of the Orbiting Carbon Observatory to the estimation of  $\text{CO}_2$  sources and sinks: theoretical study in a variational data assimilation framework, *J. Geophys. Res.*, 112, D09307, doi:10.1029/2006JD007375, 2007.

Chevallier, F., Fortems, A., Bousquet, P., Pison, I., Szopa, S., Devaux, M., and Hauglustaine, D. A.: African CO emissions between years 2000 and 2006 as estimated from MOPITT observations, *Biogeosciences*, 6, 103–111, doi:10.5194/bg-6-103-2009, 2009.

Chen, D., Wang, Y., McElroy, M. B., He, K., Yantosca, R. M., and Le Sager, P.: Regional CO pollution and export in China simulated by the high-resolution nested-grid GEOS-Chem model, *Atmos. Chem. Phys.*, 9, 3825–3839, doi:10.5194/acp-9-3825-2009, 2009.



**Variational estimates  
of black carbon  
emissions in the  
western United  
States**

Y. Mao et al.

Title Page

Abstract

Introduction

Conclusions

References

Tables

Figures

◀

▶

◀

▶

Back

Close

Full Screen / Esc

Printer-friendly Version

Interactive Discussion



- Chin, M., Ginoux, P., Kinne, S., Torres, O., Holben, B. N., Duncan, B. N., Martin, R. V., Logan, J. A., Higurashi, A., and Nakajima, T.: Tropospheric aerosol optical thickness from the GOCART model and comparisons with satellite and sun photometer measurements, *J. Atmos. Sci.*, 59, 461–483, 2002.
- 5 Chow, J. C., Watson, J. G., Pritchett, L. C., Pierson, W. R., Frazier, C. A., and Purcell, R. G.: The DRI thermal/optical reflectance carbon analysis system: description, evaluation, and applications in US air quality studies, *Atmos. Environ.*, 27, 1185–1201, 1993.
- Chow, J. C., Watson, J. G., Chen, L. W. A., Arnott, W. P., and Moosmuller, H.: Equivalence of elemental carbon by thermal/optical reflectance and transmittance with different temperature
- 10 protocols, *Environ. Sci. Technol.*, 38, 4414–4422, 2004.
- Cooke, W. F., Lioussse, C., Cachier, H., and Feichter, J.: Construction of a  $1^\circ \times 1^\circ$  fossil fuel emission data set for carbonaceous aerosol and implementation and radiative impact in the ECHAM4 model, *J. Geophys. Res.*, 104, 22137–22162, 1999.
- Dubovik, O., Lapyonok, T., Kaufman, Y. J., Chin, M., Ginoux, P., Kahn, R. A., and Sinyuk, A.: Retrieving global aerosol sources from satellites using inverse modeling, *Atmos. Chem. Phys.*, 8, 209–250, doi:10.5194/acp-8-209-2008, 2008.
- 15 Fairlie, T. D., Jacob, D. J., and Park, R. J.: The impact of transpacific transport of mineral dust in the United States, *Atmos. Environ.*, 41, 1251–1266, 2007.
- Flanner, M. G., Zender, C. S., Randerson, J. T., and Rasch, P. J.: Present-day climate forcing and response from black carbon in snow, *J. Geophys. Res.*, 112, D11202, doi:10.1029/2006JD008003, 2007.
- 20 Flanner, M. G., Zender, C. S., Hess, P. G., Mahowald, N. M., Painter, T. H., Ramanathan, V., and Rasch, P. J.: Springtime warming and reduced snow cover from carbonaceous particles, *Atmos. Chem. Phys.*, 9, 2481–2497, doi:10.5194/acp-9-2481-2009, 2009.
- 25 Fu, T.-M., Cao, J. J., Zhang, X. Y., Lee, S. C., Zhang, Q., Han, Y. M., Qu, W. J., Han, Z., Zhang, R., Wang, Y. X., Chen, D., and Henze, D. K.: Carbonaceous aerosols in China: top-down constraints on primary sources and estimation of secondary contribution, *Atmos. Chem. Phys.*, 12, 2725–2746, doi:10.5194/acp-12-2725-2012, 2012.
- 30 Fuglestedt, J. S., Shine, K. P., Bernsten, T., Cook, J., Lee, D. S., Stenke, A., Skeie, R. B., Velders, G. J. M., and Waitz, I. A.: Transport impacts on atmosphere and climate: metrics, *Atmos. Environ.*, 44, 4648–4677, 2010.

**Variational estimates  
of black carbon  
emissions in the  
western United  
States**

Y. Mao et al.

Title Page

Abstract

Introduction

Conclusions

References

Tables

Figures

◀

▶

◀

▶

Back

Close

Full Screen / Esc

Printer-friendly Version

Interactive Discussion

- Giglio, L., van der Werf, G. R., Randerson, J. T., Collatz, G. J., and Kasibhatla, P.: Global estimation of burned area using MODIS active fire observations, *Atmos. Chem. Phys.*, 6, 957–974, doi:10.5194/acp-6-957-2006, 2006.
- Giglio, L., Randerson, J. T., van der Werf, G. R., Kasibhatla, P. S., Collatz, G. J., Morton, D. C., and DeFries, R. S.: Assessing variability and long-term trends in burned area by merging multiple satellite fire products, *Biogeosciences*, 7, 1171–1186, doi:10.5194/bg-7-1171-2010, 2010.
- Gleckler, P. J., Taylor, K. E., and Doutriaux, C.: Performance metrics for climate models, *J. Geophys. Res.*, 113, D06104, doi:10.1029/2007JD008972, 2008.
- Gloor, M., Fan, S.-M., Pacala, S. W., Sarmiento, J. L., and Ramonet, M.: A model-based evaluation of inversions of atmospheric transport, using annual mean mixing ratios, as a tool to monitor fluxes of nonreactive trace substances like CO<sub>2</sub> on a continental scale, *J. Geophys. Res.*, 104, 14245–14260, 1999.
- Hack, J. J.: Parameterization of moist convection in the NCAR community climate model (CCM2), *J. Geophys. Res.*, 99, 5551–5568, doi:10.1029/93JD03478, 1994.
- Hakami, A., Henze, D. K., Seinfeld, J. H., Chai, T., Tang, Y., Carmichael, G. R., and Sandu, A.: Adjoint inverse modeling of black carbon during the Asian Pacific Regional Aerosol Characterization Experiment, *J. Geophys. Res.*, 110, D14301, doi:10.1029/2004JD005671, 2005.
- Han, S., Kondo, Y., Oshima, N., Takegawa, N., Miyazaki, Y., Hu, M., Lin, P., Deng, Z., Zhao, Y., Sugimoto, N., and Wu, Y.: Temporal variations of elemental carbon in Beijing, *J. Geophys. Res.*, 114, D23202, doi:10.1029/2009jd012027, 2009.
- Hansen, J. and Nazarenko, L.: Soot climate forcing via snow and ice albedos, *P. Natl. Acad. Sci. USA*, 101, 423–428, 2004.
- Heal, M. R.: The application of carbon-14 analyses to the source apportionment of atmospheric carbonaceous particulate matter: a review, *Anal. Bioanal. Chem.*, 406, 81–98, doi:10.1007/s00216-013-7404-1, 2014.
- Heald, C. L., Jacob, D. J., Jones, D. B. A., Palmer, P. I., Logan, J. A., Streets, D. G., Sachse, G. W., Gille, J. C., Hoffman, R. N., and Nehr Korn, T.: Comparative inverse analysis of satellite (MOPITT) and aircraft (TRACE-P) observations to estimate Asian sources of carbon monoxide, *J. Geophys. Res.*, 109, D15S04, doi:10.1029/2004JD005185, 2004.
- Hein, R., Crutzen, P. J., and Heimann, M.: An inverse modeling approach to investigate the global atmospheric methane cycle, *Global Biogeochem. Cy.*, 11, 43–76, 1997.



## Variational estimates of black carbon emissions in the western United States

Y. Mao et al.

Title Page

Abstract

Introduction

Conclusions

References

Tables

Figures

◀

▶

◀

▶

Back

Close

Full Screen / Esc

Printer-friendly Version

Interactive Discussion

transport on CO source estimates inferred from MOPITT CO retrievals, *J. Geophys. Res.-Atmos.*, 118, 2073–2083, doi:10.1002/jgrd.50216, 2013.

Jiang, Z., Jones, D. B. A., Henze, D., Worden, H., and Wang, Y. X.: Regional data assimilation of multi-spectral MOPITT observations of CO over North America, *Atmos. Chem. Phys.*, submitted, 2014a.

Jiang, Z., Jones, D. B. A., Henze, D., and Worden, H.: Sensitivity of inferred regional CO source estimates to the vertical structure in CO as observed by MOPITT, *Atmos. Chem. Phys.*, submitted, 2014b.

Jin, Y., Randerson, J. T., Faivre, N., Capps, S., Hall, A., and Goulden, M. L.: Contrasting controls on wildland fires in Southern California during periods with and without Santa Ana winds, *J. Geophys. Res.-Bioge.*, 119, 432–450, 2014.

Jones, D. B. A., Bowman, K. W., Logan, J. A., Heald, C. L., Liu, J., Luo, M., Worden, J., and Drummond, J.: The zonal structure of tropical O<sub>3</sub> and CO as observed by the Tropospheric Emission Spectrometer in November 2004 – Part 1: Inverse modeling of CO emissions, *Atmos. Chem. Phys.*, 9, 3547–3562, doi:10.5194/acp-9-3547-2009, 2009.

Kopacz, M., Jacob, D. J., Henze, D. K., Heald, C. L., Streets, D. G., and Zhang, Q.: Comparison of adjoint and analytical bayesian inversion methods for constraining Asian sources of carbon monoxide using satellite (MOPITT) measurements of CO columns, *J. Geophys. Res.*, 114, D04305, doi:10.1029/2007JD009264, 2009.

Kopacz, M., Jacob, D. J., Fisher, J. A., Logan, J. A., Zhang, L., Megretskaia, I. A., Yantosca, R. M., Singh, K., Henze, D. K., Burrows, J. P., Buchwitz, M., Khlystova, I., McMillan, W. W., Gille, J. C., Edwards, D. P., Eldering, A., Thouret, V., and Nedelec, P.: Global estimates of CO sources with high resolution by adjoint inversion of multiple satellite datasets (MOPITT, AIRS, SCIAMACHY, TES), *Atmos. Chem. Phys.*, 10, 855–876, doi:10.5194/acp-10-855-2010, 2010.

Kopacz, M., Mauzerall, D. L., Wang, J., Leibensperger, E. M., Henze, D. K., and Singh, K.: Origin and radiative forcing of black carbon transported to the Himalayas and Tibetan Plateau, *Atmos. Chem. Phys.*, 11, 2837–2852, doi:10.5194/acp-11-2837-2011, 2011.

Kopp, R. E. and Mauzerall, D. L.: Assessing the climatic benefits of black carbon mitigation, *P. Natl. Acad. Sci. USA*, 26, 11703–11708, 2010.

Korontzi, S., McCarty, J., Loboda, T., Kumar, S., and Justice, C.: Global distribution of agricultural fires in croplands from 3 years of Moderate Resolution Imaging Spectroradiometer (MODIS) data, *Global Biogeochem. Cy.*, 20, GB2021, doi:10.1029/2005GB002529, 2006.

**Variational estimates  
of black carbon  
emissions in the  
western United  
States**

Y. Mao et al.

Title Page

Abstract

Introduction

Conclusions

References

Tables

Figures

◀

▶

◀

▶

Back

Close

Full Screen / Esc

Printer-friendly Version

Interactive Discussion

- Langmann, B., Duncan, B., Textor, C., Trentmann, J., and van der Werf, G. R.: Vegetation fire emissions and their impact on air pollution and climate, *Atmos. Environ.*, 43, 107–116, 2009.
- Lee, C., Martin, R. V., van Donkelaar, A., Lee, H., Dickerson, R. R., Hains, J. C., Krotkov, N., Richter, A., Vinnikov, K., and Schwab, J. J.: SO<sub>2</sub> emissions and lifetimes: estimates from inverse modeling using in situ and global, space-based (SCIAMACHY and OMI) observations, *J. Geophys. Res.*, 116, D06304, doi:10.1029/2010JD014758, 2011.
- Levy II, H., Schwarzkopf, M. D., Horowitz, L., Ramaswamy, V., and Findell, K. L.: Strong sensitivity of late 21st century climate to projected changes in short-lived air pollutants, *J. Geophys. Res.*, 113, D06102, doi:10.1029/2007JD009176, 2008.
- Lewis, C. W., Klouda, G. A., and Ellenson, W. D.: Radiocarbon measurement of the biogenic contribution to summertime PM<sub>2.5</sub> ambient aerosol in Nashville, TN, *Atmos. Environ.*, 38, 6053–6061, 2004.
- Lin, J.-T., McElroy, M. B., and Boersma, K. F.: Constraint of anthropogenic NO<sub>x</sub> emissions in China from different sectors: a new methodology using multiple satellite retrievals, *Atmos. Chem. Phys.*, 10, 63–78, doi:10.5194/acp-10-63-2010, 2010.
- Lin, S.-J. and Rood, R. B.: Multidimensional flux-form semi-Lagrangian transport schemes, *Mon. Weather Rev.*, 124, 2046–2070, 1996.
- Liu, D. C. and Nocedal, J.: On the limited memory BFGS method for large scale optimization, *Math. Program.*, 45, 503–528, doi:10.1007/BF01589116, 1989.
- Liu, H., Jacob, D. J., Bey, I., and Yantosca, R. M.: Constraints from <sup>210</sup>Pb and <sup>7</sup>Be on wet deposition and transport in a global three-dimensional chemical tracer model driven by assimilated meteorological fields, *J. Geophys. Res.*, 106, 12109–12128, 2001.
- Martin, R. V., Jacob, D. J., Chance, K., Kurosu, T. P., Palmer, P. I., and Evans, M. J.: Global inventory of nitrogen oxide emissions constrained by space-based observations of NO<sub>2</sub> columns, *J. Geophys. Res.*, 108, 4537, doi:10.1029/2003JD003453, 2003.
- Martin, R. V., Sioris, C. E., Chance, K., Ryerson, T. B., Bertram, T. H., Wooldridge, P. J., Cohen, R. C., Neuman, J. A., Swanson, A., and Flocke, F. M.: Evaluation of space-based constraints on global nitrogen oxide emissions with regional aircraft measurements over and downwind of eastern North America, *J. Geophys. Res.*, 111, D15308, doi:10.1029/2005JD006680, 2006.
- Mao, Y. H., Li, Q. B., Zhang, L., Chen, Y., Randerson, J. T., Chen, D., and Liou, K. N.: Biomass burning contribution to black carbon in the Western United States Mountain Ranges, *Atmos. Chem. Phys.*, 11, 11253–11266, doi:10.5194/acp-11-11253-2011, 2011.

**Variational estimates  
of black carbon  
emissions in the  
western United  
States**

Y. Mao et al.

Title Page

Abstract

Introduction

Conclusions

References

Tables

Figures

◀

▶

◀

▶

Back

Close

Full Screen / Esc

Printer-friendly Version

Interactive Discussion

- Mao, Y. H., Li, Q. B., Chen, D., Zhang, L., Hao, W.-M., and Liou, K.-N.: Top-down estimates of biomass burning emissions of black carbon in the Western United States, *Atmos. Chem. Phys.*, 14, 7195–7211, doi:10.5194/acp-14-7195-2014, 2014.
- Malm, W. C., Sisler, J. F., Huffman, D., Eldred, R. A., and Cahill, T. A.: Spatial and seasonal trends in particle concentration and optical extinction in the United States, *J. Geophys. Res.*, 99, 1347–1370, 1994.
- Meirink, J. F., Bergamaschi, P., and Krol, M. C.: Four-dimensional variational data assimilation for inverse modelling of atmospheric methane emissions: method and comparison with synthesis inversion, *Atmos. Chem. Phys.*, 8, 6341–6353, doi:10.5194/acp-8-6341-2008, 2008.
- McCarty, J. L., Korontzi, S., Justice, C. O., and Loboda, T.: The spatial and temporal distribution of crop residue burning in the contiguous United States, *Sci. Total Environ.*, 407, 5701–5712, doi:10.1016/j.scitotenv.2009.07.009, 2009.
- McMurry, P. H., Shepherd, M. F., and Vickery, J. S.: *Particulate Matter Science for Policy Makers: a NARSTO Assessment*, Cambridge University Press, New York, NY, 2004.
- Mirchi, A., Madani, K., Roos, M., and Watkins, D. W.: *Climate Change Impacts on California's Water Resources, Drought in Arid and Semi-Arid Regions: a Multi-Disciplinary and Cross-Country Perspective*, Springer, Dordrecht, the Netherlands, 24, 301–319, 2013.
- Moorathi, S. and Suarez, M. J.: Relaxed Arakawa–Schubert: a parameterization of moist convection for general circulation models, *Mon. Weather Rev.*, 120, 978–1002, 1992.
- Müller, J.-F. and Stavrou, T.: Inversion of CO and NO<sub>x</sub> emissions using the adjoint of the IMAGES model, *Atmos. Chem. Phys.*, 5, 1157–1186, doi:10.5194/acp-5-1157-2005, 2005.
- Painter, T. H., Flanner, M. G., Kaser, G., Marzeion, B., VanCuren, R. A., and Abdalati, W.: End of the Little Ice Age in the Alps forced by industrial black carbon, *P. Natl. Acad. Sci. USA*, 110, 15216–15221, 2013.
- Park, R. J., Jacob, D. J., Chin, M., and Martin, R. V.: Sources of carbonaceous aerosols over the United States and implications for natural visibility, *J. Geophys. Res.*, 108, D124355, doi:10.1029/2002JD003190, 2003.
- Parrington, M., Palmer, P. I., Henze, D. K., Tarasick, D. W., Hyer, E. J., Owen, R. C., Helmig, D., Clerbaux, C., Bowman, K. W., Deeter, M. N., Barratt, E. M., Coheur, P.-F., Hurtmans, D., Jiang, Z., George, M., and Worden, J. R.: The influence of boreal biomass burning emissions on the distribution of tropospheric ozone over North America and the North Atlantic during 2010, *Atmos. Chem. Phys.*, 12, 2077–2098, doi:10.5194/acp-12-2077-2012, 2012.

## Variational estimates of black carbon emissions in the western United States

Y. Mao et al.

Title Page

Abstract

Introduction

Conclusions

References

Tables

Figures

◀

▶

◀

▶

Back

Close

Full Screen / Esc

Printer-friendly Version

Interactive Discussion

Paulot, F., Jacob, D. J., Pinder, R. W., Bash, J. O., Travis, K., and Henze, D. K.: Ammonia emissions in the United States, European Union, and China derived by high-resolution inversion of ammonium wet deposition data: interpretation with a new agricultural emissions inventory (MASAGE\_NH<sub>3</sub>), *J. Geophys. Res.-Atmos.*, 119, 4343–4364, doi:10.1002/2013JD021130, 2014.

Peterson, D. L. and Marcinkowski, K. W.: Recent Changes in Climate and Forest Ecosystems, *Climate Change and United States Forests*, Springer, Dordrecht, the Netherlands, 57, 3–11, 2014.

Pickett-Heaps, C. A., Rayner, P. J., Law, R. M., Ciais, P., Patra, P. K., Bousquet, P., Peylin, P., Maksyutov, S., Marshall, J., Rödenbeck, C., Langenfelds, R. L., Steele, L. P., Francey, R. J., Tans, P., and Sweeney, C.: Atmospheric CO<sub>2</sub> inversion validation using vertical profile measurements: analysis of four independent inversion models, *J. Geophys. Res.*, 116, D12305, doi:10.1029/2010JD014887, 2011.

Qian, Y., Gustafson Jr., W. I., Leung, L. R., and Ghan, S. J.: Effects of soot-induced snow albedo change on snowpack and hydrological cycle in western United States based on Weather Research and Forecasting chemistry and regional climate simulations, *J. Geophys. Res.*, 114, D03108, doi:10.1029/2008JD011039, 2009.

Ramana, M. V., Ramanathan, V., Feng, Y., Yoon, S.-C., Kim, S.-W., Carmichael, G. R., and Schauer, J. J.: Warming influenced by the ratio of black carbon to sulphate and the black carbon source, *Nat. Geosci.*, 3, 542–545, 2010.

Ramanathan, V. and Carmichael, G.: Global and regional climate changes due to black carbon, *Nat. Geosci.*, 1, 221–227, 2008.

Randerson, J. T., van der Werf, G. R., Giglio, L., Collatz, G. J., and Kasibhatla, P. S.: Global Fire Emissions Database, Version 2 (GFEDv2), available at: <http://daac.ornl.gov/> (last access: 2013), Oak Ridge National Laboratory Distributed Active Archive Center, Oak Ridge, Tennessee, USA, 2007.

Randerson, J. T., Chen, Y., van der Werf, G. R., Rogers, B. M., and Morton, D. C.: Global burned area and biomass burning emissions from small fires, *J. Geophys. Res.*, 117, G04012, doi:10.1029/2012JG002128, 2012.

Reche, C., Querol, X., Alastuey, A., Viana, M., Pey, J., Moreno, T., Rodríguez, S., González, Y., Fernández-Camacho, R., de la Rosa, J., Dall'Osto, M., Prévôt, A. S. H., Hueglin, C., Harrison, R. M., and Quincey, P.: New considerations for PM, Black Carbon and particle number





## Variational estimates of black carbon emissions in the western United States

Y. Mao et al.

[Title Page](#)[Abstract](#)[Introduction](#)[Conclusions](#)[References](#)[Tables](#)[Figures](#)[◀](#)[▶](#)[◀](#)[▶](#)[Back](#)[Close](#)[Full Screen / Esc](#)[Printer-friendly Version](#)[Interactive Discussion](#)

Spackman, J. R., Schwarz, J. P., Gao, R. S., Watts, L. A., Thomson, D. S., Fahey, D. W., Holloway, J. S., de Gouw, J. A., Trainer, M., and Ryerson, T. B.: Empirical correlations between black carbon aerosol and carbon monoxide in the lower and middle troposphere, *Geophys. Res. Lett.*, 35, L19816, doi:10.1029/2008GL035237, 2008.

5 Stavrakou, T. and Müller, J.-F.: Grid-based vs. big region approach for inverting CO emissions using Measurement of Pollution in the Troposphere (MOPITT) data, *J. Geophys. Res.*, 111, D15304, doi:10.1029/2005JD006896, 2006.

Subramanian, R., Kok, G. L., Baumgardner, D., Clarke, A., Shinozuka, Y., Campos, T. L., Heizer, C. G., Stephens, B. B., de Foy, B., Voss, P. B., and Zaveri, R. A.: Black carbon over Mexico: the effect of atmospheric transport on mixing state, mass absorption cross-section, and BC/CO ratios, *Atmos. Chem. Phys.*, 10, 219–237, doi:10.5194/acp-10-219-2010, 2010.

10 Szidat, S., Jenk, T. M., Synal, H.-A., Kalberer, M., Wacker, L., Hajdas, I., Kasper-Giebl, A., and Baltensperger, U.: Contributions of fossil fuel, biomass-burning, and biogenic emissions to carbonaceous aerosols in Zurich as traced by  $^{14}\text{C}$ , *J. Geophys. Res.*, 111, D07206, doi:10.1029/2005JD006590, 2006.

15 Taylor, K. E.: Summarizing multiple aspects of model performance in a single diagram, *J. Geophys. Res.*, 106, 7183–7192, 2001.

van der Werf, G. R., Randerson, J. T., Giglio, L., Collatz, G. J., Kasibhatla, P. S., and Arellano Jr., A. F.: Interannual variability in global biomass burning emissions from 1997 to 2004, *Atmos. Chem. Phys.*, 6, 3423–3441, doi:10.5194/acp-6-3423-2006, 2006.

20 van der Werf, G. R., Randerson, J. T., Giglio, L., Collatz, G. J., Mu, M., Kasibhatla, P. S., Morton, D. C., DeFries, R. S., Jin, Y., and van Leeuwen, T. T.: Global fire emissions and the contribution of deforestation, savanna, forest, agricultural, and peat fires (1997–2009), *Atmos. Chem. Phys.*, 10, 11707–11735, doi:10.5194/acp-10-11707-2010, 2010.

25 Vano, J. A., Udall, B., Cayan, D. R., Overpeck, J. T., Brekke, L. D., Das, T., and Lettenmaier, D. P.: Understanding uncertainties in future Colorado River streamflow, *B. Am. Meteorol. Soc.*, 95, 59–78, doi:10.1175/BAMS-D-12-00228.1, 2013.

Walcek, C. J., Brost, R. A., and Chang, J. S.:  $\text{SO}_2$ , sulfate and  $\text{HNO}_3$  deposition velocities computed using regional landuse and meteorological data, *Atmos. Environ.*, 20, 949–964, 1986.

30 Walker, T., Jones, D. B. A., Parrington, M., Henze, D. K., Murray, L. T., Bottenheim, J. W., Anlauf, K., Worden, J. R., Bowman, K. W., Shim, C., Singh, K., Kopacz, M., Tarasick, D. W., Davies, J., von der Gathen, P., and Carouge, C. C.: Impacts of midlatitude precursor emis-

**Variational estimates  
of black carbon  
emissions in the  
western United  
States**

Y. Mao et al.

Title Page

Abstract

Introduction

Conclusions

References

Tables

Figures

◀

▶

◀

▶

Back

Close

Full Screen / Esc

Printer-friendly Version

Interactive Discussion

sions and local photochemistry on ozone abundances in the Arctic, *J. Geophys. Res.*, 117, D01305, doi:10.1029/2011JD016370, 2012.

Wang, J., Xu, X., Henze, D. K., Zeng, J., Ji, Q., Tsay, S.-C., and Huang, J.: Top-down estimate of dust emissions through integration of MODIS and MISR aerosol retrievals with the GEOS-Chem adjoint model, *Geophys. Res. Lett.*, 39, L08802, doi:10.1029/2012GL051136, 2012.

Wang, Q., Jacob, D. J., Fisher, J. A., Mao, J., Leibensperger, E. M., Carouge, C. C., Le Sager, P., Kondo, Y., Jimenez, J. L., Cubison, M. J., and Doherty, S. J.: Sources of carbonaceous aerosols and deposited black carbon in the Arctic in winter-spring: implications for radiative forcing, *Atmos. Chem. Phys.*, 11, 12453–12473, doi:10.5194/acp-11-12453-2011, 2011.

Wang, X., Wang, Y., Hao, J., Kondo, Y., Irwin, M., Munger, J. W., and Zhao, Y.: Top-down estimate of China's black carbon emissions using surface observations: sensitivity to observation representativeness and transport model error, *J. Geophys. Res.-Atmos.*, 118, 5781–5795, doi:10.1002/jgrd.50397, 2013.

Wang, Y., McElroy, M. B., Jacob, D., and Yantosca, R. M.: A nested grid formulation for chemical transport over Asia: applications to CO, *J. Geophys. Res.*, 109, D22307, doi:10.1029/2004JD005237, 2004.

Wecht, K. J., Jacob, D. J., Wofsy, S. C., Kort, E. A., Worden, J. R., Kulawik, S. S., Henze, D. K., Kopacz, M., and Payne, V. H.: Validation of TES methane with HIPPO aircraft observations: implications for inverse modeling of methane sources, *Atmos. Chem. Phys.*, 12, 1823–1832, doi:10.5194/acp-12-1823-2012, 2012.

Westerling, A. L., Hidalgo, H. G., Cayan, D. R., and Swetnam, T. W.: Warming and earlier spring increase western US forest fire activity, *Science*, 313, 940–943, doi:10.1126/science.1128834, 2006.

Xu, B., Cao, J., Hansen, J., Yao, T., Joswia, D. R., Wang, N., Wu, G., Wang, M., Zhao, H., Wei Yang, W., Liu, X., and He, J.: Black soot and the survival of Tibetan glaciers, *P. Natl. Acad. Sci. USA*, 106, 22114–22118, 2009.

Xu, X., Wang, J., Henze, D. K., Qu, W., and Kopacz, M.: Constraints on aerosol sources using GEOS-Chem adjoint and MODIS radiances, and evaluation with Multi-sensor (OMI, MISR) data, *J. Geophys. Res.*, 118, 6396–6413, doi:10.1002/jgrd.50515, 2013.

Yumimoto, K., Uno, I., Sugimoto, N., Shimizu, A., Liu, Z., and Winker, D. M.: Adjoint inversion modeling of Asian dust emission using lidar observations, *Atmos. Chem. Phys.*, 8, 2869–2884, doi:10.5194/acp-8-2869-2008, 2008.

## Variational estimates of black carbon emissions in the western United States

Y. Mao et al.

Title Page

Abstract

Introduction

Conclusions

References

Tables

Figures

◀

▶

◀

▶

Back

Close

Full Screen / Esc

Printer-friendly Version

Interactive Discussion



Zhang, L., Jacob, D. J., Kopacz, M., Henze, D. K., Singh, K., and Jaffe, D. A.: Intercontinental source attribution of ozone pollution at western us sites using an adjoint method, *Geophys. Res. Lett.*, 36, L11810, doi:10.1029/2009gl037950, 2009.

5 Zhang, L., Jacob, D. J., Downey, N. V., Wood, D. A., Blewitt, D., Carouge, C. C., van Donkelaar, A., Jones, D. B. A., Murray, L. T., and Wang, Y.: Improved estimate of the policy relevant background ozone in the United States using the GEOS-Chem global model with  $1/2^\circ \times 2/3^\circ$  horizontal resolution over North America, *Atmos. Environ.*, 45, 6769–6776, doi:10.1016/j.atmosenv.2011.07.054, 2011.

10 Zhang, Y., Jaeglé, L., van Donkelaar, A., Martin, R. V., Holmes, C. D., Amos, H. M., Wang, Q., Talbot, R., Artz, R., Brooks, S., Luke, W., Holsen, T. M., Felton, D., Miller, E. K., Perry, K. D., Schmeltz, D., Steffen, A., Tordon, R., Weiss-Penzias, P., and Zsolway, R.: Nested-grid simulation of mercury over North America, *Atmos. Chem. Phys.*, 12, 6095–6111, doi:10.5194/acp-12-6095-2012, 2012.

15 Zhu, L., Henze, D. K., Cady-Pereira, K. E., Shephard, M. W., Luo, M., Pinder, R. W., Bash, J. O., and Jeong, G.-R.: Constraining US ammonia emissions using TES remote sensing observations and the GEOS-Chem adjoint model, *J. Geophys. Res. Atmos.*, 118, 3355–3368, doi:10.1002/jgrd.50166, 2013.

Zwally, H. J., Abdalati, W., Herring, T., Larson, K., Saba, J., and Steffen, K.: Surface melt-induced acceleration of Greenland ice-sheet flow, *Science*, 297, 218–222, 2002.

20 Zyrichidou, I., Koukoulis, M. E., Balis, D., Markakis, K., Kioutsioukis, I., Poupkou, A., Melas, D., Boersma, K. F., and van Roozendael, M.: Compilation of a  $\text{NO}_x$  emission inventory for the Balkan region using satellite tropospheric  $\text{NO}_2$  columns, *Advances in Meteorology, Climatology and Atmospheric Physics*, 1265–1271, 2013.

Variational estimates of black carbon emissions in the western United States

Y. Mao et al.

Title Page

Abstract Introduction

Conclusions References

Tables Figures

◀ ▶

◀ ▶

Back Close

Full Screen / Esc

Printer-friendly Version

Interactive Discussion

**Table 1.** Monthly biomass burning and anthropogenic emissions of BC (Gg) in the western US for August 2006.

|              | Inversions    | Emissions                  | Biomass burning (Gg)     |                    |                       |                         | Anthropogenic (Gg) | Total (Gg) |            |
|--------------|---------------|----------------------------|--------------------------|--------------------|-----------------------|-------------------------|--------------------|------------|------------|
|              |               |                            | The Rockies <sup>a</sup> | CA & the Southwest | The Pacific Northwest | Total                   |                    |            |            |
| A priori     |               |                            | 1.3                      | 0.5                | 1.0                   | 2.8                     | 5.8                | 8.6        |            |
| A posteriori | Analytical    | 2° × 2.5° <sup>c</sup>     | 7.6                      | 1.4                | 0.9                   | 9.9 (3.5 <sup>b</sup> ) | 2.8 (0.5)          | 12.7 (1.5) |            |
|              |               | 0.5° × 0.667° <sup>d</sup> | 4.1                      | 0.1                | 1.9                   | 6.1 (2.7)               | 3.1 (0.5)          | 9.1 (1.1)  |            |
| A posteriori | Adjoint       | Case 1 <sup>e</sup>        | 3.0                      | 1.4                | 1.5                   | 5.9 (2.1)               | 11.8 (2.0)         | 17.7 (2.1) |            |
|              |               | Case 2 <sup>f</sup>        | 2.9                      | 1.3                | 1.4                   | 5.6 (2.0)               | 11.6 (2.0)         | 17.2 (2.0) |            |
|              |               | Case 3 <sup>g</sup>        | 3.2                      | 1.4                | 1.6                   | 6.2 (2.2)               | 11.4 (2.0)         | 17.6 (2.0) |            |
|              |               | 2° × 2.5°                  | Case 4 <sup>h</sup>      | 3.3                | 1.5                   | 1.7                     | 6.5 (2.3)          | 12.8 (2.2) | 19.3 (2.2) |
|              |               | Case 5 <sup>i</sup>        | 2.4                      | 1.2                | 1.0                   | 4.6 (1.7)               | 10.3 (1.8)         | 14.9 (1.7) |            |
|              |               | Case 6 <sup>j</sup>        | 2.8                      | 1.3                | 1.4                   | 5.5 (2.0)               | 11.1 (1.9)         | 16.6 (1.9) |            |
|              |               | Case 7 <sup>k</sup>        | 3.1                      | 1.4                | 1.5                   | 6.0 (2.1)               | 11.6 (2.0)         | 17.6 (2.0) |            |
|              | 0.5° × 0.667° | Case 8 <sup>l</sup>        | 2.2                      | 0.8                | 2.3                   | 5.3 (1.9)               | 8.6 (1.5)          | 13.9 (1.6) |            |

<sup>a</sup> See Fig. 3.1 in Mao et al. (2014) for the geographical definitions of the BC source regions.  
<sup>b</sup> Scaling factors are in parentheses.  
<sup>c</sup> The standard analytical inversion at 2° × 2.5° (Mao et al., 2014). The uncertainties are 50% for anthropogenic emissions (S<sub>a</sub>ANTH = 50%) and 500% for biomass burning emissions (S<sub>a</sub>BB = 500%), and the observation error is 30% (S<sub>z</sub> = 30%). See text for details.  
<sup>d</sup> Same as (c), except at 0.5° × 0.667° (Mao et al., 2014).  
<sup>e</sup> The standard adjoint inversion at 2° × 2.5°. Same error specifications as (c).  
<sup>f</sup> Same as (e), except with S<sub>a</sub>BB = 300%.  
<sup>g</sup> Same as (e), except with S<sub>a</sub>ANTH = 30%.  
<sup>h</sup> Same as (e), except with S<sub>a</sub>ANTH = 200%.  
<sup>i</sup> Same as (e), except with S<sub>z</sub> = 100%.  
<sup>j</sup> Same as (e), except with only 56 sites. See text for details.  
<sup>k</sup> Same as (e), except with the a priori biomass burning emissions uniformly increased by 2.5 Mg in every model grid box.  
<sup>l</sup> Same as (e), except at 0.5° × 0.667°.



## Variational estimates of black carbon emissions in the western United States

Y. Mao et al.

Title Page

Abstract

Introduction

Conclusions

References

Tables

Figures

◀

▶

◀

▶

Back

Close

Full Screen / Esc

Printer-friendly Version

Interactive Discussion



**Table 2.** Monthly anthropogenic and biomass burning emissions of BC (Gg) in the western US from the adjoint inversions for August 2006 using pseudo observations.

| Inversions                     | A posteriori | Emissions (Gg)          |                 | $\Delta$ Emissions (Gg) | $J(X)$ reduction (%) |
|--------------------------------|--------------|-------------------------|-----------------|-------------------------|----------------------|
|                                |              | Anthropogenic           | Biomass burning |                         |                      |
| Pseudo 1 <sup>a</sup>          |              | 7.7 (1.3 <sup>j</sup> ) | 6.5 (2.3)       | 5.6 (2.0 <sup>k</sup> ) | 95                   |
| Pseudo 2 <sup>b</sup>          |              | 7.8 (1.3)               | 6.4 (2.3)       | 5.6 (2.0)               | 97                   |
| Pseudo 3 <sup>c</sup>          |              | 7.1 (1.2)               | 6.9 (2.5)       | 5.4 (1.9)               | 95                   |
| Pseudo 4 <sup>d</sup>          |              | 5.8 (1.0)               | 8.2 (2.9)       | 5.4 (1.9)               | 99                   |
| Pseudo 5 <sup>e</sup>          |              | 10.0 (1.7)              | 2.8 (1.0)       | 4.2 (1.5)               | 55                   |
| Pseudo 6 <sup>f</sup>          |              | 7.8 (1.3)               | 6.2 (2.2)       | 5.4 (1.9)               | 94                   |
| Pseudo 7 <sup>g</sup>          |              | 8.0 (1.4)               | 5.9 (2.1)       | 5.3 (1.9)               | 93                   |
| Pseudo 8 <sup>h</sup>          |              | 7.8 (1.3)               | 5.3 (1.9)       | 4.5 (1.6)               | 96                   |
| “Ghost” emissions <sup>i</sup> |              | 5.8 (1.0)               | 8.4 (3.0)       | 5.6 (2.0)               |                      |
| A priori                       |              | 5.8                     | 2.8             |                         |                      |

<sup>a</sup> Pseudo observations in every surface grid box.

<sup>b</sup> Same as (a), except with pseudo observations in the lowest 15 layers over each grid box.

<sup>c</sup> Same as (a), except with  $S_a$ ANTH = 10 %.

<sup>d</sup> Same as (a), except that anthropogenic emissions are shut off.

<sup>e</sup> Same as (a), except that biomass burning emissions are shut off.

<sup>f</sup> Same as (a), except with pseudo observations (randomly) in 75 % of the surface grid boxes.

<sup>g</sup> Same as (a), except with pseudo observations (randomly) in 50 % of the surface grid boxes.

<sup>h</sup> Same as (a), except with pseudo observations (randomly) in 25 % of the surface grid boxes.

<sup>i</sup> Emissions (with anthropogenic emissions unchanged but biomass burning emissions tripled) used to generate the pseudo observations.

<sup>j</sup> Scaling factors in parentheses.

<sup>k</sup> Ratio of the total emissions change (increase) over the a priori biomass burning emissions.

## Variational estimates of black carbon emissions in the western United States

Y. Mao et al.

Title Page

Abstract

Introduction

Conclusions

References

Tables

Figures

◀

▶

◀

▶

Back

Close

Full Screen / Esc

Printer-friendly Version

Interactive Discussion

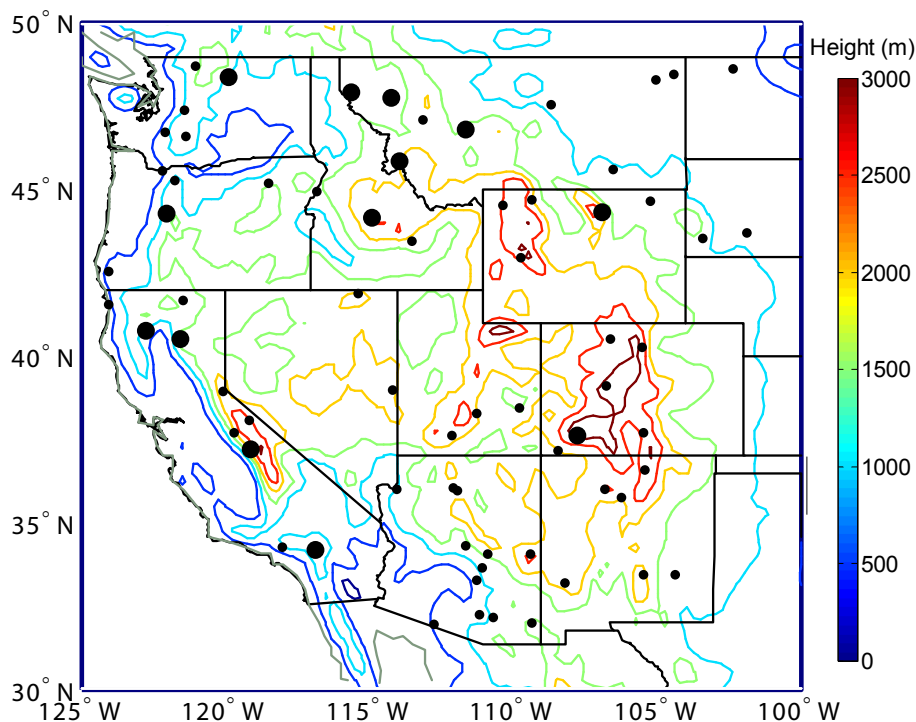


**Figure 1.** IMPROVE sites (solid circles; data available at <http://vista.cira.colostate.edu/improve/>) in the western US Also shown are terrain heights (color contours).

**Variational estimates  
of black carbon  
emissions in the  
western United  
States**

Y. Mao et al.

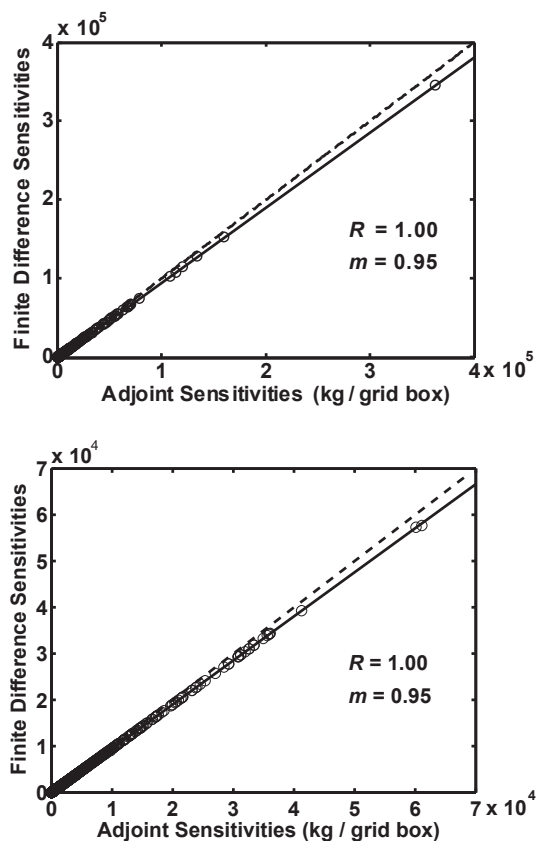


**Figure 2.** Sensitivities of surface BC mass to the scaling factors of BC emissions as computed using GEOS-Chem adjoint and the finite difference approximation (Eq. 1). Results are from 1 week simulations for biomass burning (top panel) and anthropogenic emissions (bottom panel) for August 2006. Dashed lines are 1 : 1 and solid lines are regression lines.

[Title Page](#)[Abstract](#)[Introduction](#)[Conclusions](#)[References](#)[Tables](#)[Figures](#)[◀](#)[▶](#)[◀](#)[▶](#)[Back](#)[Close](#)[Full Screen / Esc](#)[Printer-friendly Version](#)[Interactive Discussion](#)

## Variational estimates of black carbon emissions in the western United States

Y. Mao et al.

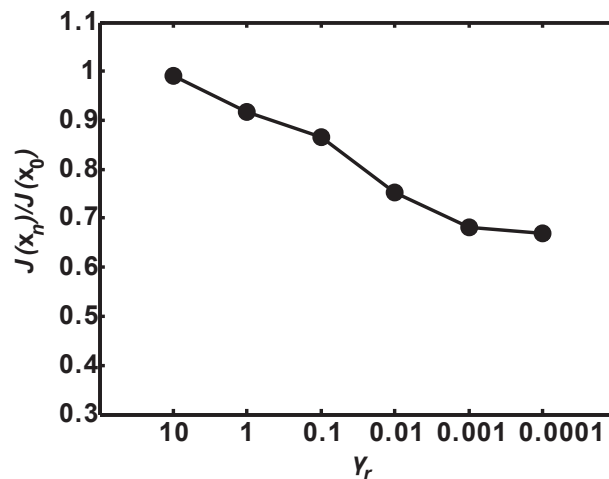


**Figure 3.** Normalized a posteriori cost function  $J(X_n)/J(X_0)$  as a function of the regularization parameter  $\gamma_r$  (Eq. 3) for August 2006.

[Title Page](#)[Abstract](#)[Introduction](#)[Conclusions](#)[References](#)[Tables](#)[Figures](#)[◀](#)[▶](#)[◀](#)[▶](#)[Back](#)[Close](#)[Full Screen / Esc](#)[Printer-friendly Version](#)[Interactive Discussion](#)



**Variational estimates  
of black carbon  
emissions in the  
western United  
States**

Y. Mao et al.

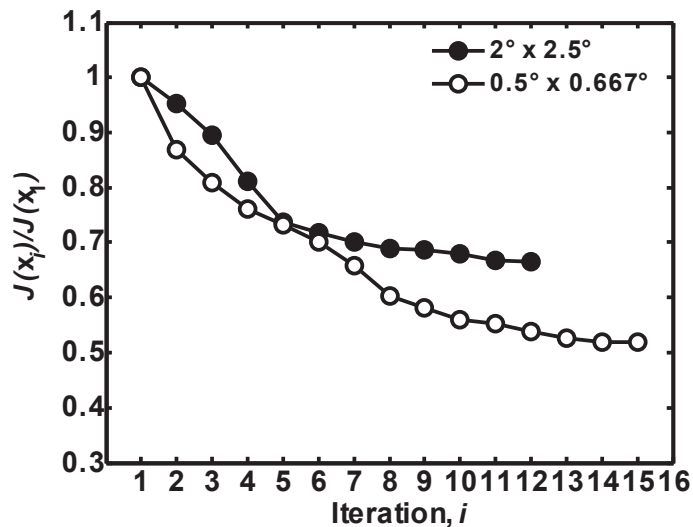


**Figure 4.** Reduction in the normalized cost function  $J(X_i)/J(X_0)$  at  $2^\circ \times 2.5^\circ$  and  $0.5^\circ \times 0.667^\circ$  for August 2006.

[Title Page](#)[Abstract](#)[Introduction](#)[Conclusions](#)[References](#)[Tables](#)[Figures](#)[◀](#)[▶](#)[◀](#)[▶](#)[Back](#)[Close](#)[Full Screen / Esc](#)[Printer-friendly Version](#)[Interactive Discussion](#)

Variational estimates  
of black carbon  
emissions in the  
western United  
States

Y. Mao et al.

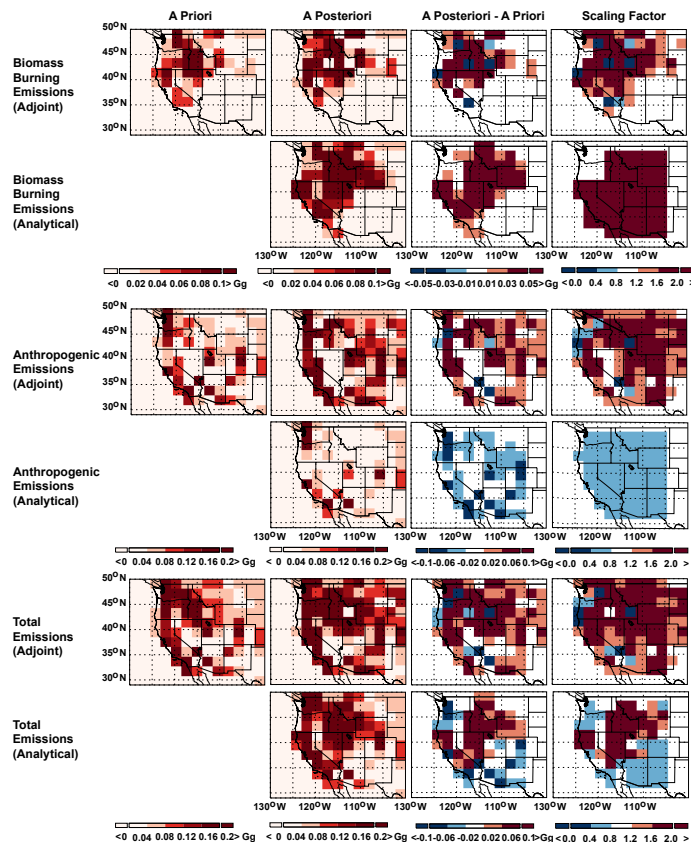


**Figure 5.** Emissions of BC in the western US for August 2006: (top two rows) biomass burning, (middle two rows) anthropogenic, and (bottom two rows) total emissions. First column: the a priori; second column: the optimized inventory; third column: differences between the a posteriori and a priori; fourth column: scaling factors. Retrieval results are from the standard adjoint (Case 1, Table 1) and analytical (Mao et al., 2014) inversions at  $2^\circ \times 2.5^\circ$ .

Variational estimates of black carbon emissions in the western United States

Y. Mao et al.

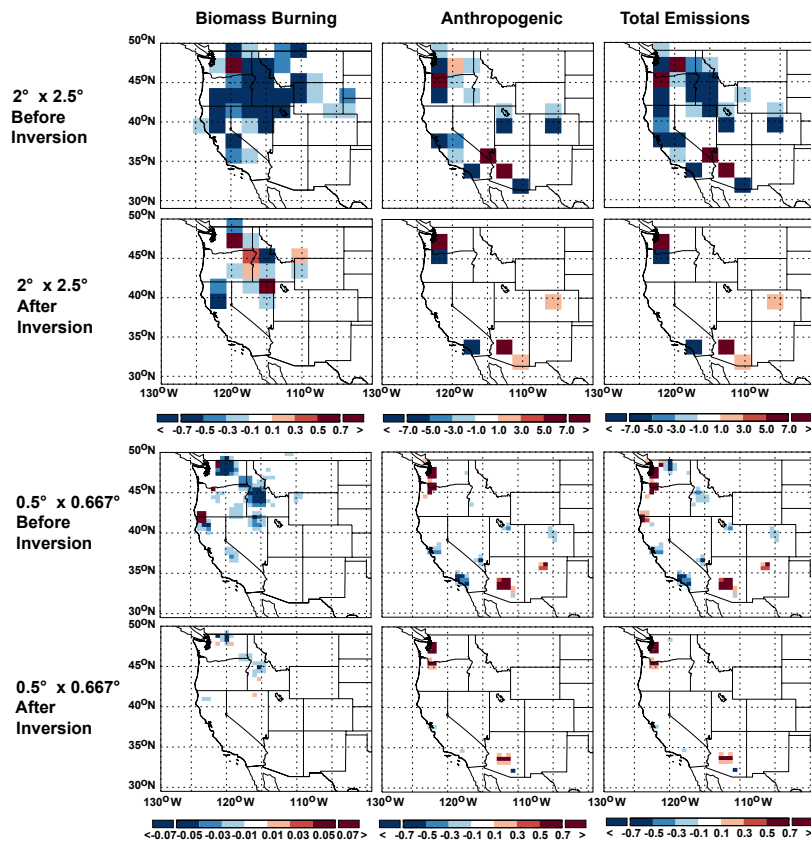


**Figure 6.** Normalized sensitivities of the cost function with respect to the BC emissions (left: biomass burning BC; middle: anthropogenic BC; right: total emissions of BC) before and after the inversions at  $2^\circ \times 2.5^\circ$  (Case 1, Table 1) and  $0.5^\circ \times 0.667^\circ$  (Case 8) for August 2006.

Title Page

Abstract Introduction

Conclusions References

Tables Figures

◀ ▶

◀ ▶

Back Close

Full Screen / Esc

Printer-friendly Version

Interactive Discussion



Variational estimates of black carbon emissions in the western United States

Y. Mao et al.

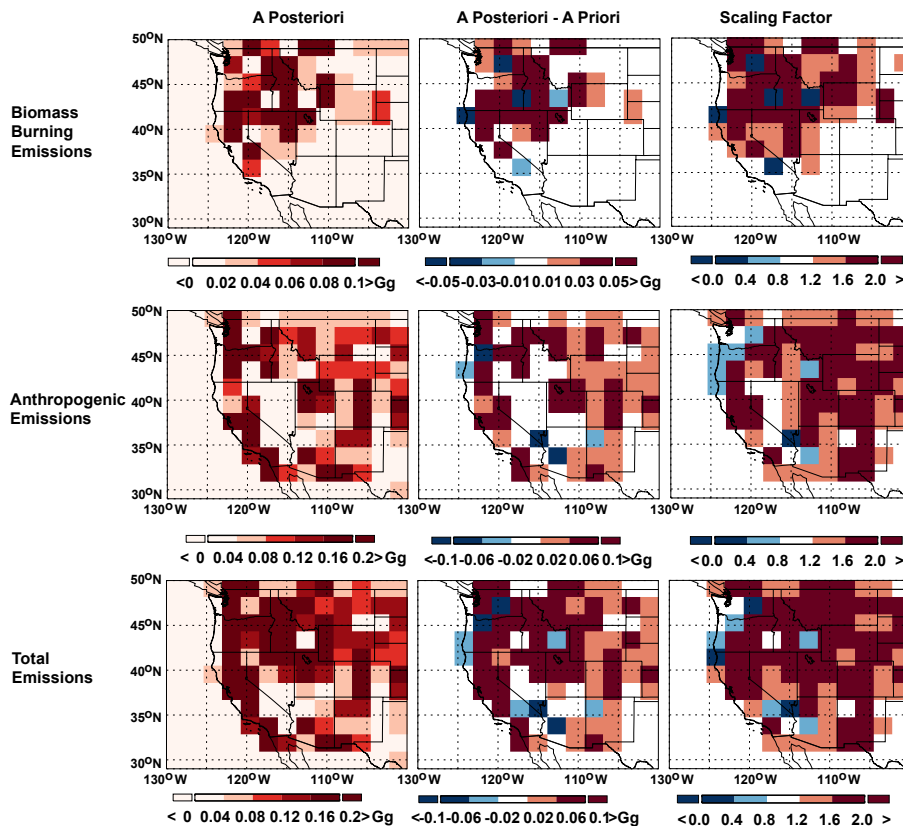


**Figure 7.** Emissions of BC in the western US for August 2006: (top panels) biomass burning, (middle panels) anthropogenic, and (bottom panels) total emissions. Results are from Case 6 (Table 1): (left column) the optimized inventory, (middle column) a posteriori-a priori, and (right column) the scaling factors.

|                          |              |
|--------------------------|--------------|
| Title Page               |              |
| Abstract                 | Introduction |
| Conclusions              | References   |
| Tables                   | Figures      |
| ◀                        | ▶            |
| ◀                        | ▶            |
| Back                     | Close        |
| Full Screen / Esc        |              |
| Printer-friendly Version |              |
| Interactive Discussion   |              |



## Variational estimates of black carbon emissions in the western United States

Y. Mao et al.

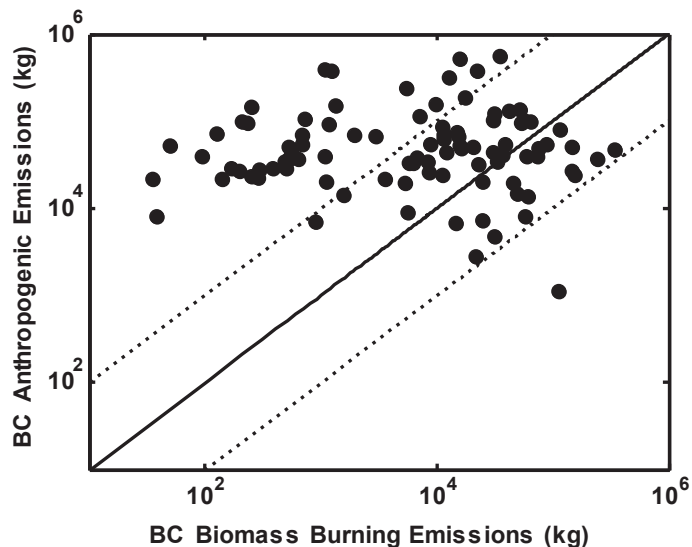


**Figure 8.** Monthly anthropogenic and biomass burning emissions of BC in each  $2^\circ \times 2.5^\circ$  grid box for August 2006 (kg). Solid line is 1 : 1 and dashed lines are 1 : 10 (or 10 : 1).

Title Page

Abstract

Introduction

Conclusions

References

Tables

Figures

◀

▶

◀

▶

Back

Close

Full Screen / Esc

Printer-friendly Version

Interactive Discussion

Variational estimates of black carbon emissions in the western United States

Y. Mao et al.

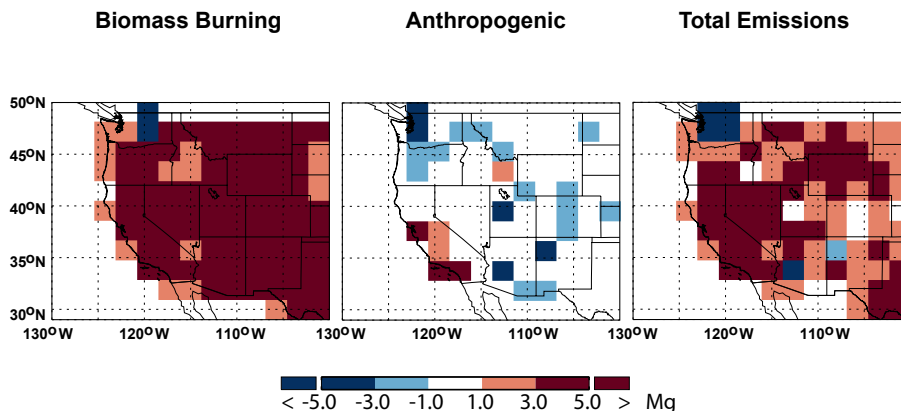


Figure 9. Emissions of BC: Case 7 minus Case 1 (Table 1) at  $2^\circ \times 2.5^\circ$  for August 2006.

Title Page

Abstract

Introduction

Conclusions

References

Tables

Figures

◀

▶

◀

▶

Back

Close

Full Screen / Esc

Printer-friendly Version

Interactive Discussion



## Variational estimates of black carbon emissions in the western United States

Y. Mao et al.

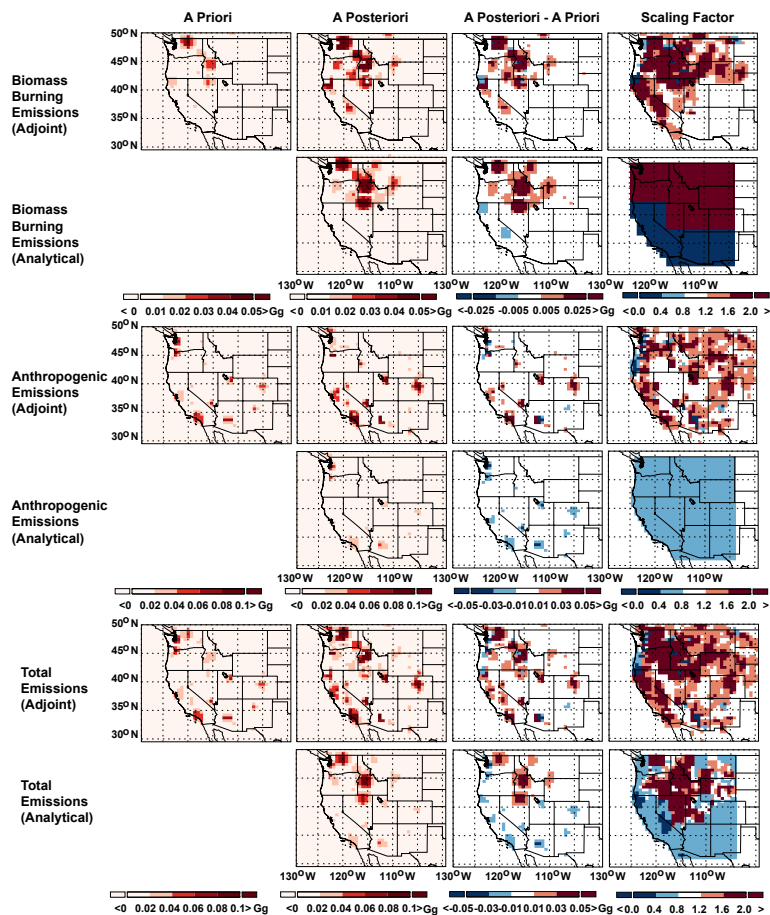


Figure 10. Same as Fig. 5, but at  $0.5^\circ \times 0.667^\circ$  (Case 8, Table 1).

Title Page

Abstract

Introduction

Conclusions

References

Tables

Figures

◀

▶

◀

▶

Back

Close

Full Screen / Esc

Printer-friendly Version

Interactive Discussion

## Variational estimates of black carbon emissions in the western United States

Y. Mao et al.

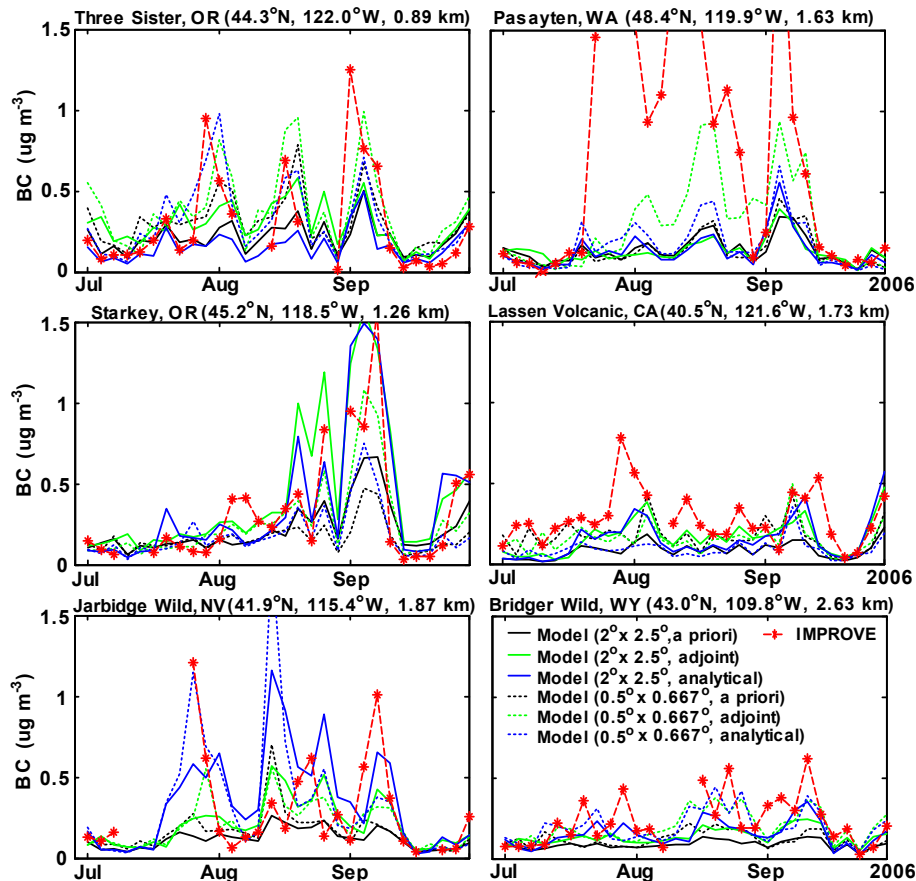


**Figure 11.** Observed (red line) and GEOS-Chem simulated 24 h average surface BC concentrations ( $\mu\text{g m}^{-3}$ ) at six IMPROVE sites for July–September 2006. Results are for  $2^\circ \times 2.5^\circ$  (solid) and  $0.5^\circ \times 0.667^\circ$  (dotted line) with the a priori (black line) or a posteriori emissions from the analytical (blue line) or adjoint (green line) inversions.



## Variational estimates of black carbon emissions in the western United States

Y. Mao et al.

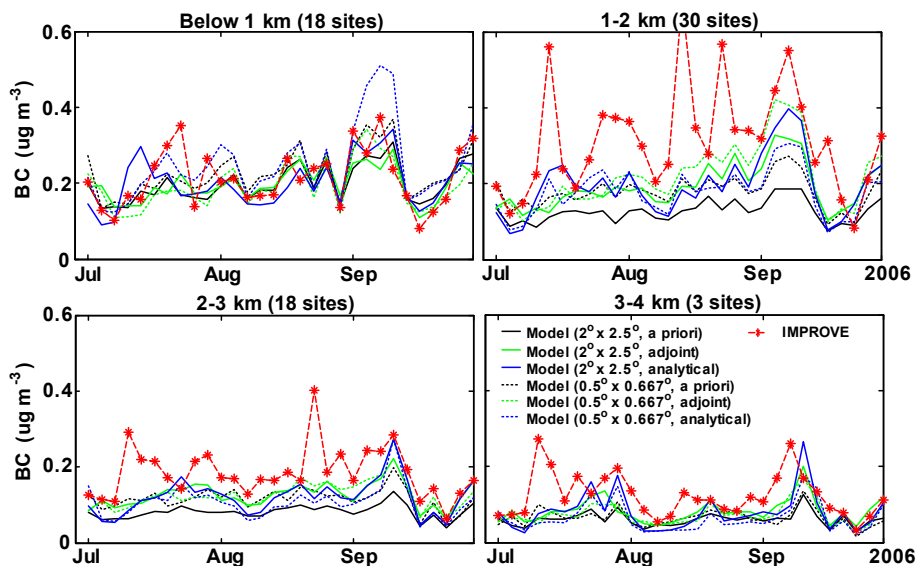


**Figure 12.** Observed (red line) and GEOS-Chem simulated 24 h average surface BC concentrations ( $\mu\text{g m}^{-3}$ ) for July–September 2006, averaged for the IMPROVE sites (Fig. 1) in altitudes below 1 km, 1–2 km, 2–3 km, and above 3 km (3 sites). Results are for  $2^\circ \times 2.5^\circ$  (solid line) and  $0.5^\circ \times 0.667^\circ$  (dotted line) with the a priori (black line) or a posteriori emissions from the analytical (blue line) or adjoint (green line) inversions.

[Title Page](#)
[Abstract](#)
[Introduction](#)
[Conclusions](#)
[References](#)
[Tables](#)
[Figures](#)
[◀](#)
[▶](#)
[◀](#)
[▶](#)
[Back](#)
[Close](#)
[Full Screen / Esc](#)
[Printer-friendly Version](#)
[Interactive Discussion](#)

## Variational estimates of black carbon emissions in the western United States

Y. Mao et al.

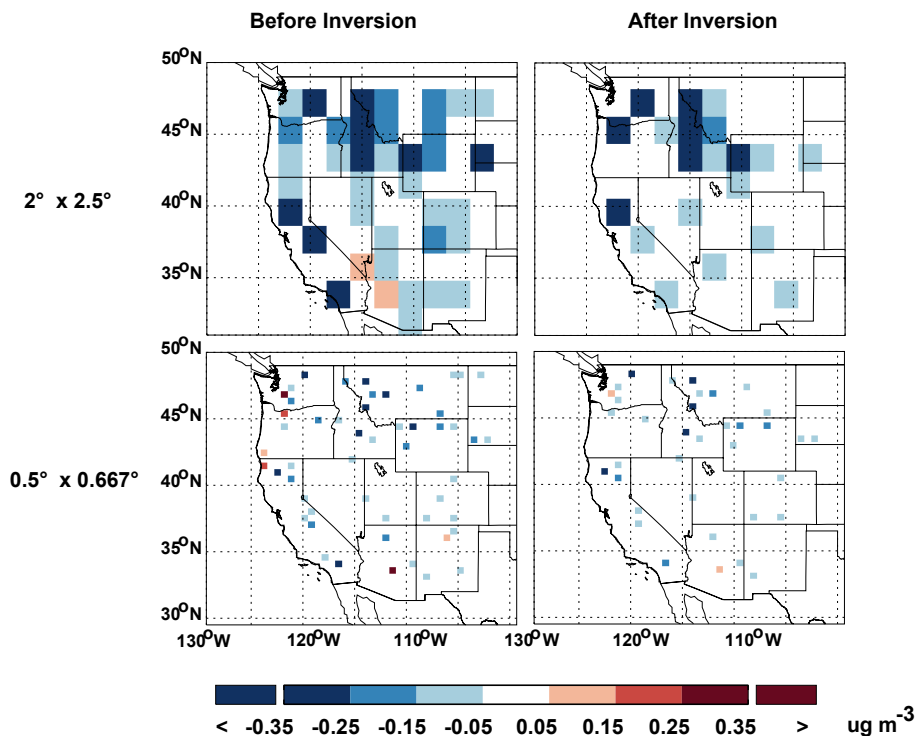


**Figure 13.** Differences between GEOS-Chem simulated and observed 24 h average surface BC concentrations at the 69 IMPROVE sites (Fig. 1) for August 2006. Model results are from the adjoint inversions at  $2^\circ \times 2.5^\circ$  (Case 1, Table 1) and  $0.5^\circ \times 0.667^\circ$  (Case 8) with the a priori or a posteriori emissions.

[Title Page](#)
[Abstract](#)
[Introduction](#)
[Conclusions](#)
[References](#)
[Tables](#)
[Figures](#)
[◀](#)
[▶](#)
[◀](#)
[▶](#)
[Back](#)
[Close](#)
[Full Screen / Esc](#)
[Printer-friendly Version](#)
[Interactive Discussion](#)

## Variational estimates of black carbon emissions in the western United States

Y. Mao et al.

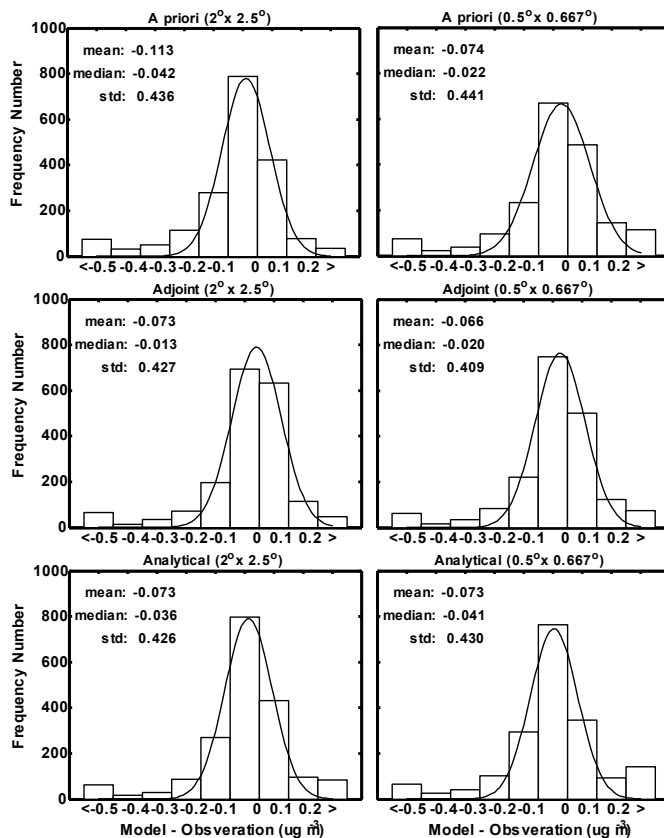


**Figure 14.** Frequency distribution of the bias of GEOS-Chem simulated 24 h average surface BC concentrations for July–September 2006. Results are for  $2^\circ \times 2.5^\circ$  and  $0.5^\circ \times 0.667^\circ$  with the a priori or a posteriori emissions from the analytical or adjoint inversions. Also shown are the mean, median, standard deviation, and fitted Gaussian distribution.

Variational estimates of black carbon emissions in the western United States

Y. Mao et al.

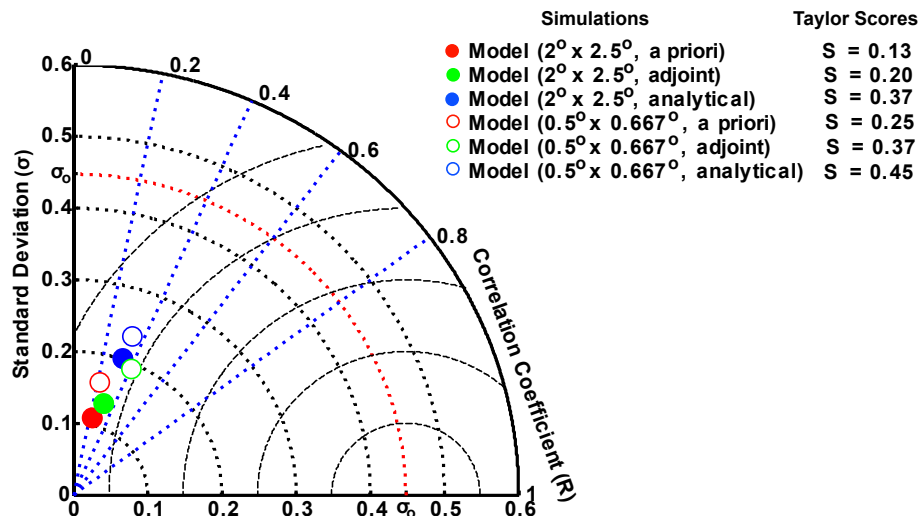


**Figure 15.** Taylor diagram and Taylor scores for GEOS-Chem simulations of BC for July–September 2006 at  $2^\circ \times 2.5^\circ$  (solid circle) and  $0.5^\circ \times 0.667^\circ$  (open circle) with the a priori (red circle) or a posteriori emissions from the analytical (blue circle) or adjoint (green circle) inversions. Values are averages for the 69 IMPROVE sites (Fig. 1).

Title Page

Abstract Introduction

Conclusions References

Tables Figures

◀ ▶

◀ ▶

Back Close

Full Screen / Esc

Printer-friendly Version

Interactive Discussion

